Sensor Placement and Graphical User Interface for Photovoltaic Array Monitoring System

by

Venkatachalam Krishnan

A Thesis Presented in Partial Fulfillment
of the Requirements for the Degree
Master of Science

Approved February 2012 by the
Graduate Supervisory Committee:

Andreas Spanias, Co-Chair
Cihan Tepedelenlioglu, Co-Chair
Raja Ayyanar
Antonia Papandreou-Suppappola

ARIZONA STATE UNIVERSITY

May 2012

ABSTRACT

With increased usage of green energy, the number of photovoltaic arrays used in power generation is increasing rapidly. Many of the arrays are located at remote locations where faults that occur within the array often go unnoticed and unattended for large periods of time. Technicians sent to rectify the faults have to spend a large amount of time determining the location of the fault manually. Automated monitoring systems are needed to obtain the information about the performance of the array and detect faults. Such systems must monitor the DC side of the array in addition to the AC side to identify non catastrophic faults.

This thesis focusses on two of the requirements for DC side monitoring of an automated PV array monitoring system. The first part of the thesis quantifies the advantages of obtaining higher resolution data from a PV array on detection of faults. Data for the monitoring system can be gathered for the array as a whole or from additional places within the array such as individual modules and end of strings. The fault detection rate and the false positive rates are compared for array level, string level and module level PV data. Monte Carlo simulations are performed using PV array models developed in Simulink and MATLAB for fault and no fault cases. The second part describes a graphical user interface (GUI) that can be used to visualize the PV array for module level monitoring system information. A demonstration GUI is built in MATLAB using data obtained from a PV array test facility in Tempe, AZ. Visualizations are implemented to display information about the array as a whole or individual modules and locate faults in the array.

ACKNOWLEDGEMENTS

This document represents not just my work but also the contributions of several people. This work would not be possible without the guidance and support I received from them.

I wish to thank my advisors Prof. Cihan Tepedelenlioglu and Prof. Andreas Spanias for their constant support and evaluation of my work. Their technical expertise and insight helped me become a better researcher and complete this work. I thank ‘Paceco corporation’ for providing the opportunity to work on their project and for the financial support which helped me immensely during my Masters. I would like to thank Mr.Ted Yeider from Paceco for helping me with design ideas for the GUI and reviewing my work. I am grateful to Prof. Raja Ayyanar and Prof. Antonia Papandreou-Suppappola for taking the time to review my thesis and being a part of my committee.

I would like to thank all my friends and colleagues in the signal processing research groups for their invaluable assistance. Special thanks to Dr. Mahesh Banavar who reviewed all my writing work and Henry Braun and Tejasri Buddha who reviewed all my research work. Finally, I would like to thank all my friends for their support and my parents for their faith in me.

TABLE OF CONTENTS

CHAPTER Page

LIST OF TABLES

LIST OF FIGURES

Figure Page

Chapter 1

INTRODUCTION

This chapter discusses the motivation for this research and the contributions of this work.

1.1 Motivation

The thrust towards clean energy has resulted in increase in the number of photovoltaic (PV) arrays. Photovoltaic arrays are very low efficiency systems and convert only a fraction of the solar energy incident on them into electricity. Performance analysis of a 342kW roof mounted PV array using 10 years of data showed the array operating with an efficiency of 7-9 percent [1]. Hence there is a need to increase the output of PV arrays by all means. The efficiencies of inverters which convert the direct current generated by the modules into alternate current are already close to maximum. A recent PV inverter from Advanced Energy Industries achieves a conversion efficiency of 99 percent [2]. Therefore no significant gains are possible from improving inverter efficiency. Alternately, PV array outputs can be increased by improving the efficiency of the PV modules. A survey done in 2004 showed that the median value of efficiency of crystalline silicon PV modules was close to 12.5 percent [3,4]. Improving efficiencies through better materials is an important field [5]. However improving efficiency in materials might take years of research. Another way to improve PV array output is to ensure that the array operates in optimal output conditions at all times. PV arrays once installed are expected to operate with minimal human intervention. However, a PV array can perform well below its optimum output power levels due to faults in modules, wiring, inverter etc. Most of these faults remain undetected for long periods of time resulting in loss of power. Technicians sent to locate and fix the faults within a array need to take time consuming field measurements. Automated monitoring systems that capture the state of the array and apply signal processing techniques to the data

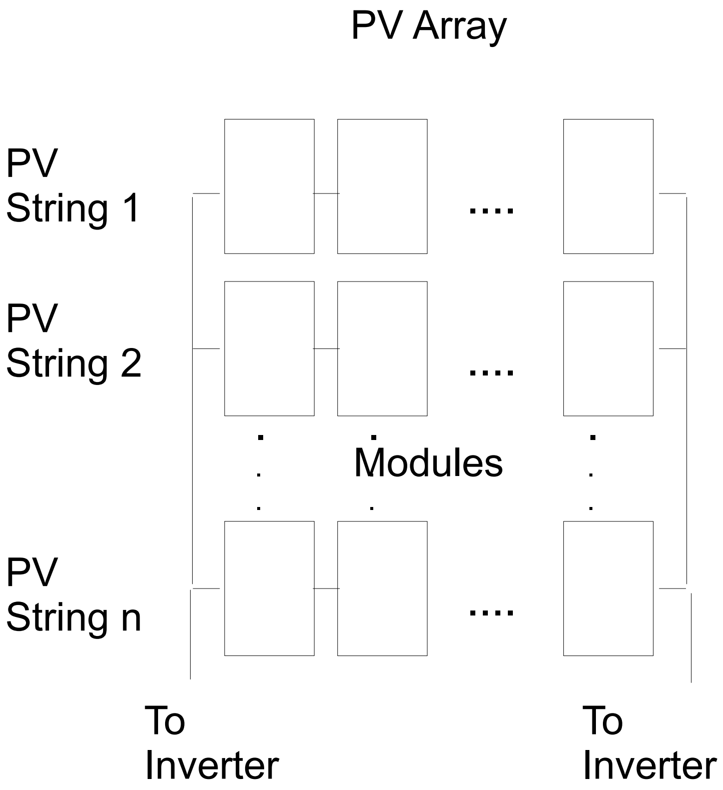

Figure 1.1: Electrical connection of modules in an array.

obtained can improve fault detection and provide information to help the technicians narrow down the location of the problem. This results in increased uptime of the array and improves PV efficiency.

PV arrays convert solar radiation incident on them to electricity. They are composed of several components such as PV modules, inverters and electrical connections. The block diagram of a typical PV array is shown in Figure 1.1. PV modules in the same row are connected electrically in series to increase the generated voltage. This series arrangement is called a string. To form the array, several strings are connected in parallel thereby increasing the current generated. The DC power generated by the array is converted to AC by means of an inverter.

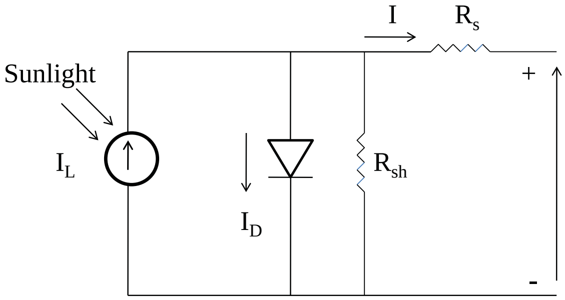

Figure 1.2: Single-diode model of a PV module.

The output current and voltage of a solar module depends on several factors such as module temperature, irradiance (amount of solar radiation power incident per square area), angle of incidence of the sun and spectrum of the incoming light [6–8]. A solar module is often modelled as a current source in parallel with a diode, with parasitic series and shunt resistance [9–11] as shown in Figure 1.2. As with the diode, we can characterize the behavior of the PV module by its current-voltage relationship. I_L is the light generated current and it depends mainly on the irradiance. Hence the PV module generates more current at higher irradiance values. The voltage across the diode depends mainly on the module temperature and the PV module outputs higher voltage at lower temperatures.

The current voltage (I-V) characteristics of a PV module operating at standard test conditions of 1000 W/m^2 irradiance and 25 degrees celcius temperature is shown in Figure 1.3. V_{OC} and I_{SC} represent the open circuit and the short circuit conditions respectively. For a given set of environmental conditions, the solar module has a voltage and current (V_{MP}, I_{MP}), at which it produces its maximum power P_{MP}. Modern inverters dynamically adjust the load they present to a solar array in order to maintain operation near P_{MP} using a process known as maximum power point tracking (MPPT) [12–15].

For an ideal PV array, the power output is the sum of the power generated by each of the modules. However, PV array performance can be reduced significantly in

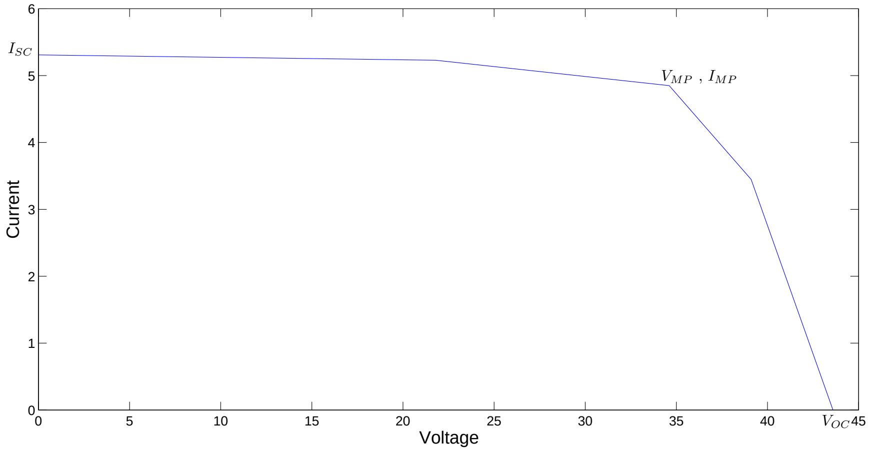

Figure 1.3: I-V curve of a PV module at standard test conditions.

.

the presence of faults. Several types of faults such as module mismatch [16], soiling [17], shading [18–20], ground faults [21] and arc faults [22, 23] occur in PV arrays.

The series-parallel topology commonly employed in PV arrays implies that every module in a string must carry the same current. As a result, faults in a single module would result in a sub-optimal operating point for all the modules in a string, leading to a higher loss of power. For instance, it is shown in [24] that a partial shadow on a single string can result in a loss of power corresponding to over 30 times its physical size. Hence, any fault in the array must be identified as soon as possible. Since the output of the PV array depends on environmental conditions which vary over time, faults can go undetected if only the output power of the array is measured. This results in need for automated monitoring systems that can identify faults.

Most PV monitoring systems collect information on the AC side of the array. The monitored parameters typically are the AC voltage, current and frequency. This type of monitoring will be able to identify any catastrophic faults that affect the output of the array significantly. Faults such as shading of a few modules within the array cannot be detected from the AC side. To detect those faults we need monitoring on the DC side as well. Parameters to measure on the DC side include DC voltage and current at the inverter, string/module voltages and currents and module temperatures. Additionally, weather information from the site such as irradiance, temperature and wind speed can be measured. PV models such as the Sandia model [25] can be used to predict the output of the modules/ array. The predicted values can be compared against measured values to detect faults. Hence monitoring systems for DC side monitoring of a PV array need to be investigated.

A DC side monitoring system for PV array must consider several factors essential for effective array management such as

- Parameters to measure. These include electrical parameters such as voltages and currents and weather parameters such as irradiance, temperature and wind speed.
- Locations within the array to measure the parameters. These include DC side input to the inverter, the end of each string and individual modules.
- Central server for processing the obtained information from within the array.
- Communication systems to transfer the data from measurement sensors to server. These can be wireless, ethernet or power line communication systems.
- Algorithms to process the data. This includes fault detection algorithms and PV models to calculate array expected outputs.
- Visualization tools to make sense of the data.

This work tries to address two of these factors. The location of sensors within the array is studied by comparing their ability to detect faults within the array. The visualization of data is studied using a demonstration GUI built for an experimental PV array.

1.2 Objective

The objectives of this thesis are twofold. The first part of this thesis quantifies the effect of higher resolution PV array data on detection of faults within the array. Models of PV modules and arrays were developed using Simulink. The models were used to obtain array outputs for faulty conditions (such as shading and ground faults) and normal operating conditions. Model mismatch and measurement noise were added to the simulations. The Simulink model outputs were compared against expected values obtained using Sandia PV array performance model; outputs that differ by more than a specific threshold were classified as faulty. Thresholds were obtained by running the simulations on non faulty data and fixing specific false alarm rates. The same thresholds were used in the simulations of faulty data and the detection thresholds for array, string and module level sensing systems were identified. The fault detection performance of each type of monitoring system is compared for false alarm rates identified earlier. The second part of the thesis analyzes the requirements for a graphical user interface (GUI) for module level monitoring of a PV array. A demonstration GUI was developed in MATLAB using data obtained from a module level PV array monitoring system in Tempe, Arizona. Several displays were built to illustrate how the information obtained from the array can be used to provide insight in to the array's health. Displays built include fault detection displays which run statistics based clustering algorithms to identify faulty modules, array maps which pinpoint the location of the module in the array and module display which compares each module's actual output against expected output from models.

1.3 Contributions of the Thesis

The contributions of this research are

- Quantifying the fault detection rate for array, string, and module level DC monitoring systems for ground faults and shading affecting one or more modules.
- Simulation and analysis of array, string, and module level DC monitoring system performance in detecting faults for fixed false alarm rates.

- Data visualizations for PV array monitoring systems that sense voltage and current at each module.

- Demonstration GUI for PV array monitoring systems that illustrates visualizations for array, module outputs and fault detection algorithms.

1.4 Organization of the Thesis

This thesis is organised as follows. Chapter 2 talks about the need for an automated monitoring system and discusses the requirements for a PV monitoring system. Chapter 3 shows the simulation results for the different sensor configurations. The fault detection capabilities of each sensor system is studied for a 52 module array and the results are tabulated. Chapter 4 talks about graphical user interface features for module level monitoring of a PV array. A demonstration GUI built in MATLAB is described and its various features are explained. Chapter 5 presents the conclusions and future work.

Chapter 2

MONITORING PV ARRAYS

This chapter explains the need for an automated PV array monitoring system, some existing methods of PV monitoring and discusses the different sub-systems required for DC side monitoring.

2.1 The Need for AC Side Monitoring

PV arrays require effective monitoring on the AC side of the inverter to help the utility company maintain power quality, obtain information about outages and adhere to standards for connecting PV to the grid.

Prevent Outages

The power output of PV systems, unlike traditional fossil fuel based generation schemes depends on factors such as solar irradiance, cloud cover and temperature [25]. The power output of the array might drop or increase drastically at any instant in time depending on external factors. Sudden drops in output power from large PV plants could lead to power outages [26]. As PV achieves higher grid penetration, a centralized monitoring system becomes essential. Such a system would allow greater control over the contribution of specific PV plant to the grid. If the PV plant with a monitoring system has reduced output, controllers would be able to supplement the power with traditional systems such as a storage battery or a diesel electric plant.

Islanding Protection

The addition of arrays to the power grid poses a safety risk known as islanding. Islanding occurs when a fault in the wider electrical grid causes a power outage, but a PV array does not turn off. This might result in the PV array supplying the local loads resulting in the formation of a small ‘island’ in the grid. This island of energized wires poses a threat to repair technicians seeking to fix the fault. Modern inverters are, for the most part, equipped with anti-islanding features which detect when the AC grid goes down and shut off the inverter. In addition to this safeguard, many electrical companies require that residential arrays connected to their grid come equipped with a manual disconnect switch, to be opened by a power company technician before beginning work on nearby parts of the grid.

The IEEE standard 1547 [26] provides guidelines for interconnecting a distributed generation resource (such as PV) with power systems. The standard provides guidelines such as bounds on voltage and frequency distortion while laying out response requirements to abnormalities. The guidelines mandate that the PV array interconnection system must detect unintentional islanding and cease to energize the electric power system. The standard mandates that if the aggregate of the distributed resources at a single point of common coupling (point where a local electric power system is connected to an area electric power system) equals or exceeds 250kVA, there must be provisions to monitor the connection status, power output and voltage at the point of distributed resource connection.

Improve Power Quality

Power utility companies are responsible for ensuring power quality. Significant deviation in the magnitude, frequency or purity of waveforms results in power quality problems. The utility has no control over the amount of current a load might draw. Power quality is maintained by keeping the voltage and frequency within certain limits. The output of PV arrays vary significantly over time resulting in potential power quality problems. Monitoring and control of PV arrays can be used improve power quality by changing the outputs such as voltage and frequency of a PV array.

The availability of monitoring information from various distributed sources in a given area can provide better insight for the electric power company. This information provides avenues for better understanding of a given area and means to improve power quality. As more PV is added to the grid, power quality becomes a serious concern.

Performance Evaluation

Effective monitoring of a PV array can be used to evaluate the performance of the array. For instance, the voltage and currents generated by the array can be used to determine the annual energy production. This can then be used to determine the cost per watt of the PV system. The electrical outputs such as power generated can be compared to the weather data using PV models to determine the efficiency of operation of the system.

2.2 The Need for DC side monitoring

Monitoring on the AC side of the array cannot be used to determine the location of the faults if any within a PV array. PV arrays require monitoring on the DC side to identify faulty modules, calculate the efficiency of operation of the modules and determine long term/ short term trends of the system.

Identify Faults

Methods of fault detection that rely only on human operators are not accurate and might result in faults remaining unnoticed. Automated monitoring systems must be used to identify the presence of faults in an array or sub-array. Monitoring on the AC side cannot detect faults that affect only a few modules in the array. The loss of power due to such a fault is indistinguishable from measurement errors and seasonal variations. Hence, monitoring is required on the DC side to detect faults effectively. For instance, [27] suggests an ad-hoc methods that utilizes information obtained at the end of each string to identify faults that reduce the string output by over 20 percent. Automated monitoring systems can use sophisticated signal processing algorithms to identify the exact location of the fault within the array. A signal processing algorithm that utilizes measurements from each module to detect ground fault and arc fault locations at over 99 percent accuracy is described in [28].

Evaluating Trends

The outputs collected on the DC side can be compared to the historical data to determine the long term trends. For instance, module data collected from previous years can be compared with that of the current year to calculate the module degradation factor. The output of the modules can be compared to weather data to update PV models.

2.3 Existing Methods of Monitoring

Several systems have already been developed to monitor PV arrays and modules. We look into some of these systems currently being used emphasising systems that perform intra-array monitoring. The usability of each system varies depending on their targeted capabilities.

A monitoring system used to evaluate the performance of PV array installed on a building is given in [29]. The monitoring system measures voltage, current and power at the AC output of the inverter. It measures the solar intensity using two photo diode sensors and taking their average. Module internal temperatures are obtained using temperature sensors. The measurements are done over 20 minute intervals. The data can be used for both short term purposes such as monitoring the system's status, and long term purposes such as monitoring the deterioration of components. Comparison of the different strings helps evaluate the effect of shading on the array. The correlation of output power with temperature can be used to determine the effect of module temperature on output power for the same irradiance. These measurements can be used to evaluate the annual energy production and cost of electricity produced by the array. Measurements are transferred to a computer enabling internet access to the data. The authors mention the use of commercially available data acquisition systems to transfer the data to the computer. Here, the monitoring system does not consider module level measurements and communication systems for such an arrangement.

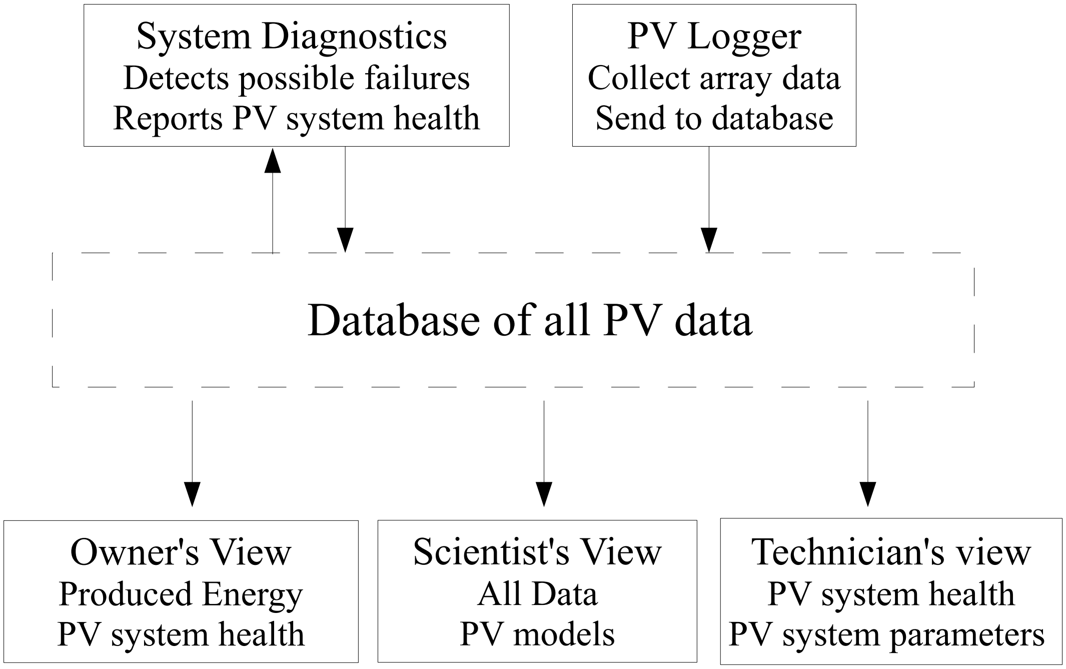

Figure 2.1: Schematic for data access according to the need of each user.

Kolodenny et.al [30] propose an approach that uses modern informatics tools such as XML to analyze the acquired data. Their goal is to analyse the performance of a PV system of any type and size. They propose a protocol called PV mark up language (developed from XML) to automatically access, extract and use data from several sensors systems/database sources. The system collects and classifies the data. Depending on whether the user is a technician or plant owner or scientist, different views are presented containing only the most relevant information. Figure 2.1 shows the schematic for their data access system. A PV logger system constantly collects information about the state of the array (such as voltages, currents and irradiance) and updates it in a database. The system diagnostics retrieves the data and detects possible failures. This information is then updated in the database. The different users can query the database and obtain information they are interested in. The owner can view the overall system health and output of the array while the technician can view the PV system parameters. The scientist's view provides access to all the data collected including the PV system models. This work provides a comprehensive method to store and retrieve PV array data and can be used with different current voltage sensor location and weather data. However, it does not describe a complete PV monitoring system which includes sensing, data communication and user interface systems.

A simple and cost effective method of monitoring a PV power station using a GUI built in NI LabVIEW is presented in [31]. The set-up consists of current sensors for each string and voltage sensor for the array connected to a micro-controller through an analog multiplexer. Irradiance is measured using a pyranometer. Also included are sensors for measuring the module surface temperature. The collected data can be used for both monitoring and control. The micro-controller is interfaced to a laptop through a serial port where the data can be viewed and analyzed using a GUI designed using LabVIEW. The GUI provides views for PV array output and battery health and calculates PV expected outputs using the diode equivalent model given in Figure 1.2. This system does not consider module level sensor networks and communication systems for them.

2.4 Monitoring System Considerations

Each monitoring system discussed in the previous section addresses specific aspects of PV array monitoring such as data acquisition, data management and graphical user interface. These different aspects of a PV monitoring have to be combined in a single automated system.

The block diagram for a PV array with an automated monitoring system is shown in Figure 2.2. The PV modules are connected to the inverter to form the PV array. Sensors are placed to collect the PV currents and voltages from the DC input to inverter, end of each string and/or individual modules. The measured parameters are transmitted to the central server through a communication channel. The communication channels used can be ethernet, wireless or power line. A weather station records the irradiance and temperature values and transmits them to the central server. The central server maintains a database of the array outputs and weather data. It runs PV models to

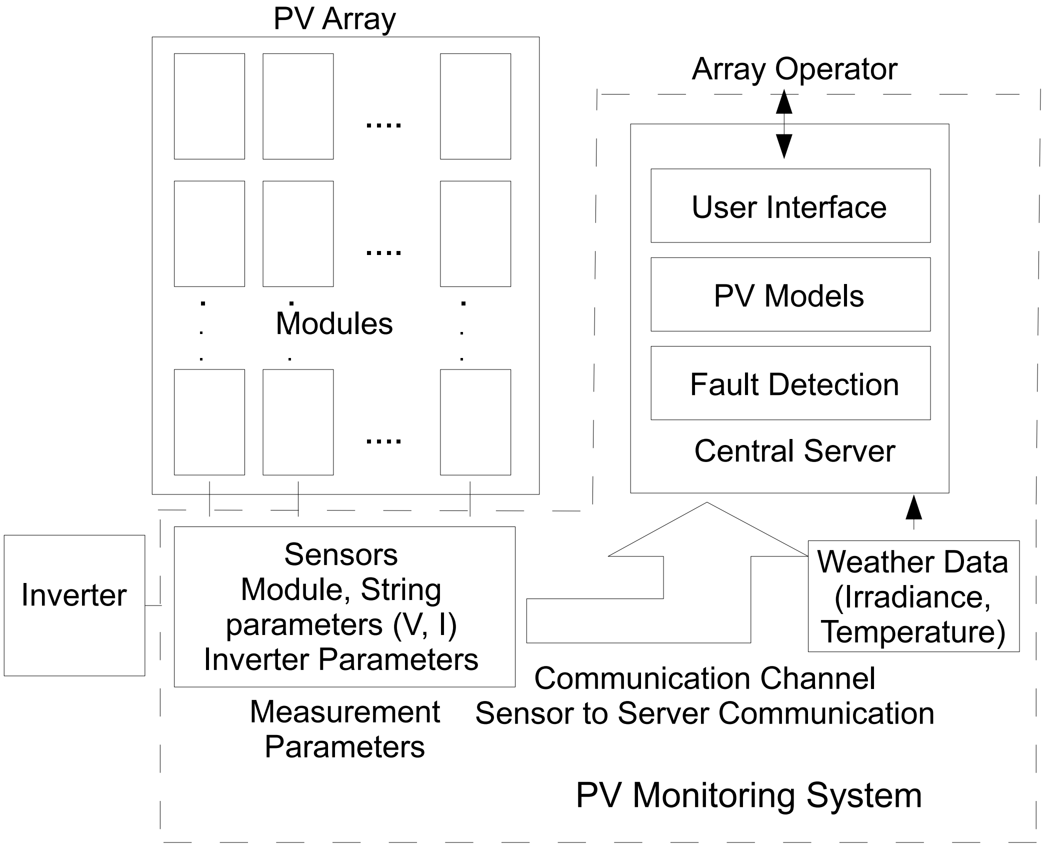

Figure 2.2: Block diagram of a PV array with automated monitoring system.

calculate expected output values and fault detection algorithms to detect the presence of faults in the array. The array operator has access to the expected and actual output and fault information through an easy to use GUI.

There are several aspects to be considered for an effective monitoring system for PV arrays. These include the parameters to be measured, the placement of sensors for measuring these parameters, communication systems that can transfer the measurements to a central database, algorithms to manage and process the collected data and user interfaces to visualize the state of the PV arrays. This section discusses these aspects briefly.

Sensor Measurements

PV array characteristics can be determined from the measured parameters such as voltage, current and irradiance. The measurements of current and voltage can be made at different locations such as the array, end of each string and each module.

Most currently used PV monitoring systems, record current and voltage measurements at the inverter to analyze the performance of the array. Using the data for a typical year at the site and models such as the Sandia performance model [25], the expected output power of the array can be calculated. These can be compared with the actual power output by the inverter to determine whether the array is operating without any faults. For example, using monthly averaged energy at the inverter as a metric, loss of energy in the array was identified and rectified in [25]. Inverter faults are characterised by large variation between expected and actual AC power while actual and expected DC powers remain similar. Array faults are characterised by significant variation between expected and actual DC power.

Though measurements at the inverter level enable us to identify the overall health of the system, they cannot in most cases detect non catastrophic faults. They do not provide enough information to identify the location and nature of faults immediately. Identifying and correcting a fault or under performing component in the array still involves taking field measurements by technicians. Higher resolution data acquired by means of additional sensors installed on individual modules or strings provides more precise understanding of the array. These sensors can measure module or string currents and voltages and identify modules to be inspected in case of fault.

It is possible to measure the temperature, wind-speed and irradiance at the installation site. Approximate estimates of the module cell temperature can be estimated from the atmospheric temperature and wind speed [25]. These can be used in models for PV arrays to predict the output of the PV array. Significant differences between

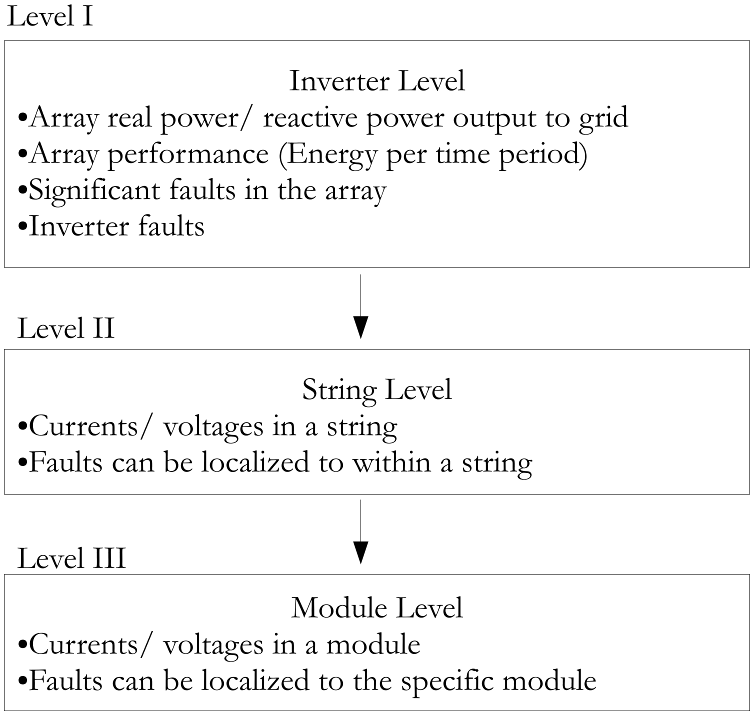
Level I
Inverter Level
•Array real power/ reactive power output to grid
•Array performance (Energy per time period)
•Significant faults in the array
•Inverter faults
Level II
String Level
•Currents/ voltages in a string
•Faults can be localized to within a string
Level III
Module Level
•Currents/ voltages in a module
•Faults can be localized to the specific module

Figure 2.3: Levels of measurement in a PV array : inverter, strings and modules.

the predicted outputs and actual measurements can be utilized in an automated fault detection set-up.

The measurements at string level provide a more definitive description of the performance of an array when compared to only inverter level measurements. However they are far from perfect. Cell temperatures calculated from atmospheric temperature do not reflect the exact temperatures of the cells required for use in the PV models. This can be due to manufacturing process variations, wiring effects and other factors such as high resistance connections. Even cells within a single module might have variation in their temperatures. Better estimates of cell temperature may be acquired by sensors on the back surface of modules. These module level measurements can then be used in conjunction with the string level and inverter level measurements. The different measurement levels for a PV array and their capabilities are summarized in Figure 2.3. As the number of measurement points increases, the automatic monitoring system becomes more effective in localizing the faults.

Increasing the number of measurement points would increase the complexity of the monitoring system. Since there is just a single point of data collection for inverter level monitoring, transmitting the data to a server for processing is relatively straightforward. Monitoring at the string and module level requires a distributed network of sensors. These must be able to transmit the information collected to either the central server themselves or transmit the information among one another until it reaches a gateway sensor node which can transmit to the central server. The following section discusses technologies to transfer the data from the sensors to the server.

Sensor to Server Communication

Measurement of currents and voltages at the module level or string level provides better analysis and control capabilities. But this requires effective methods to transmit the sensor information to a central server for processing. The central server can be located at the site of the PV array and analysis or data transfer to the grid level monitoring systems can be performed from this server. The data rate requirements for monitoring systems scale linearly with the size of the array, and inversely with the sampling period of the measurement sensors. To avoid clutter associated with the transfer of data through wires, wireless technologies can be used. Individual sensors would require relatively low data bandwidth to transfer the measurements to the server. The power consumption for the data transfer must be low to enable extended use of the sensors in the field without battery replacements. The requirements of low power and low data rate makes wireless technologies such as variants of IEEE 802.15.4.2006 (Zigbee, WirelessHART) and in some cases Ultra-wideband (UWB) practical. Data communication for PV systems can also utilize power line communications (PLC) which would utilize the existing infrastructure to transfer the data across power lines to the inverter. Any data transfer mechanism can be used to transmit this data collected at a single point to the server. A brief description of PLC and wireless systems is given below.

To avoid extra wiring, or interference with existing devices, PLC technologies [32, 33] can be used for communications. PLC is widely used both over high-voltage and low-voltage lines. However there is no adopted IEEE standard, especially in the context of PV arrays. Communication of data on the DC generation side of the PV array can make use of protocols such as RS 232 [34]. The PLC channel introduces large amounts of time and frequency variation in the medium of propagation. The time-variation of the communication medium is due to sudden electrical load changes which alter the overall impedance of the system. The frequency variation is due to the dispersive nature of the medium which causes reflections of the transmitted waveform.

Using wireless technologies to transmit the data from the sensors to the server can be considered as an alternative to PLC. ZigBee [35] is a wireless standard which is an extension of the IEEE 802.15.4.2006 standard focussing on low cost, low power communication between devices located within a typical range of 10 - 75 metres. The data rates are in the order of kilobits per second, which is sufficient to transmit the array state to the server or the gateway sensor. ZigBee utilizes significantly lower power compared to standards such as Wi-Fi and Bluetooth.

Ultra wide band (UWB) communication is a wireless technology that can be used if the distance between the transmitter and receiver is extremely small (around 10 m). UWB communications consume low power and transmit information without affecting other systems using the same frequency band. However, UWB can handle much higher bandwidth than ZigBee. UWB communications do not have any security protocols whereas the ZigBee uses encryption.

These wireless technologies for data communication of the PV system suffer from some of the same problems as that of PLC. These might include interference from other wireless devices, signal distortions in the form of time-dispersion and signal fading.

There is no standard that dictates the usage of these technologies in the PV area. It is advantageous to have PLC communication over ZigBee when the data rates are low (in the order of hundreds of bits per second) and the coverage requirements of the network are more than the range of ZigBee (say over 100 metres). ZigBee is better suited for data rates in the order of kilobits per second and a smaller coverage area.

User Interface

Once the sensors and the communication systems to the server are set up, there is a need for algorithms and user interfaces that enable the user to make sense of the data and take appropriate actions. Simple and easy to use GUIs need to be developed for visualizing solar array data. Such GUIs can provide information on overall health of the system. They are linked to sophisticated data processing algorithms and models of PV systems and can be used to evaluate the PV array performance, detect failures etc.

The GUI must provide a real time update of the current state of operation of the array. This includes the AC/DC power output generated by the array, faults if any detected and the status of the battery. It can include other information such as real/ reactive power output to the grid, total power output during the day/week/month and the yield/efficiency of operation. The cost of power generated can be displayed. This is especially useful for residential PV arrays as owners can keep track of the effective amount earned from their array after energy consumption for their residence.

The GUI can provide comprehensive tools to analyze the array as a whole or individual modules, strings etc. Fault detection algorithms can be used to display the nature and location of any faulty modules. The GUI can provide tools to plot/analyze the array/module output against weather data such as irradiance. This can be done for current day or across several days using stored data and can be used to study the short term and long term trends in the array.

The GUI should be connected to other systems such as audible alarms to alert the operator when faults occur. They can be connected to emergency systems such as fire or flood alert systems as required. They can be integrated with perimeter security systems such as video cameras to provide a single point of reference for the human operator. If required, a PV monitoring system GUI must be able to enforce data security based on access privileges.

2.5 Summary

This chapter discussed the need for monitoring systems for photovoltaic arrays. Such monitoring systems should be able to provide the system operator with information regarding the array's operation. The level of detailed data collected from a PV array determines the accuracy and capabilities of the monitoring system. Monitoring systems with higher resolution data from the DC side of the array can be used to identify faults in the array. The considerations for designing such a monitoring system includes the location and placement of sensors, the communication system to be used for transmitting the data to a server, the algorithms used for processing the data collected from the array and the user interface that lets the operator visualize and take actions based on the data.

Chapter 3

COMPARISON OF SENSOR CONFIGURATION PERFORMANCE IN DETECTING FAULTS

This chapter describes the simulation set-up for PV monitoring system with array, string and module level monitoring information and compares their relative performance in identifying faults within the array. First, the types of faults in a PV array are described followed by the PV models used in the simulation, the metrics used to compare the different configurations and the results.

Monitoring systems collect the voltages and current outputs several times a day. As seen in Chapter 2, typical monitoring systems only collect the output power at the inverter while some systems might collect the currents and voltages at both the DC and AC side of the inverter. Additionally, the monitoring system might have access to historical output values and weather data. This information is used to calculate the expected output for the array and compare it against actual output to determine the health of the array. Faults that result in reduction in output power by few percentage points can be confused with seasonal variation. Expected values calculated from weather data have uncertainties associated with them due to errors in irradiance measurements and modelling mismatch. Faults that affect only a few modules in the array cannot be detected because of these uncertainties. Even when faults are detected, determining the exact location of the fault is a time consuming process.

The fault detection performance of the PV array monitoring system can be improved by taking measurements of currents and voltages within the array. Data gathering from the array can be done at the end of each string or at each module. The output at these additional data points can be compared to expected values obtained from the weather data. This results in smaller faults within the array being identified. String level monitoring information can detect faults when only a few modules in a given string are affected by the fault. Module level monitoring can detect faults for even a single module affected case. Additionally these methods can determine the location of the fault within the array reducing the time to repair.

In this work, the monitoring system which collects data only at the array level (DC input to inverter) is compared against systems that collect data at each module and the end of each string. The comparison is done based on the ability of the monitoring system to detect faults within the array. The fault types considered are ground faults and shading that affect one or more modules.

3.1 Faults in PV Array

PV array normal operation can be affected by the presence of faults that reduce can power output and cause potential damage to the array. This section describes some of the faults that occur in PV arrays.

Inverter Fault

Inverters are generally considered to be the weakest link in a PV array [36, 37]. Reliability of an inverter is the product of the reliability of all its components. Inverters have several components such as IGBTs, capacitors and drive circuitry and failure of even one component can result in inverter failure. Inverter failures are the worst kind of faults that can occur with respect to array power output. This is because the array can continue to operate when PV modules fail but inverter failure shuts down the entire array.

Ground Fault

Ground fault occurs when there is a path from any point in the array to ground. This results in reduction of array voltage and power and is a serious threat to personnel. Depending on the location point of the fault, the output of one or more modules are affected. Ground fault circuit interrupters which can detect leakage currents caused by the fault and open a switch to stop the flow of current. Utility inverters are mandated by United States National Electric Code (NEC) [21] to have ground fault interruption functionality. Individual PV modules are grounded to protect personnel, however the standard does not mandate individual PV modules and strings to have ground fault circuit interrupters.

Shading

Shading occurs when part or the entire sunlight reaching a PV module is blocked. This occurs due to the presence of trees, overhead power lines or nearby buildings. Shading causes a reduction in the current output by the module. Additionally it affects the output of other healthy modules in the array. When the shaded module is connected in series with healthy modules, the current in the entire string gets reduced. Though PV modules contain bypass diodes that can bypass the module entirely in the case of severe shading, the other modules in the string have to compensate for the loss of voltage by operating away from their maximum power points. Shading can be a serious issue depending on the number of modules shaded and the duration of the day for which the shading occurs.

Arc Fault

Arc fault is a spark across the air and can be serious in PV arrays [23, 38, 39]. It can occur as a series or parallel arc. Series arcs can occur when any connection breaks between modules or within modules resulting in two conductors near each other. Parallel arcs can occur when two conductors of different voltages are close to one another and the insulation between them is faulty. Arc faults can result in serious damage to the array and even cause fires.

3.2 Simulation Setup

A PV array is modelled in Simulink using the five parameter circuit model presented in [11]. Current and voltage sensors are placed for the array as a whole, individual modules and individual strings. PV array data for normal operating conditions is obtained by simulating the model with irradiance and temperature measurements for an entire day. PV array data for faulty conditions is obtained by reducing irradiance values (shading) of individual modules and shorting individual modules to ground (ground fault). The Sandia array performance model [25] is used to generate the expected values to compare with the data obtained. Model mismatch and measurement noise for the sensors are added. Monte Carlo simulations are performed with the normal operating condition data to obtain the fault detection thresholds for different false alarm rates. The same thresholds are used on Monte Carlo simulations of faulty array data to obtain detection rates. The different sensing methods are compared based on the fault detection rates for fixed false alarm rates.

Five Parameter Model

The five parameter model is used to model the behavior of a PV module. This model provides a method to calculate the parameters of the PV module circuit model shown in Figure 1.2 from the manufacturer's data sheet specifications. The model utilizes only the data provided by the manufacturer such as open circuit voltage (V_{OC}), short circuit current (I_{SC}), maximum power point voltage and current (V_{MP}, I_{MP}) at standard test conditions. Using this information, the five parameters used in the circuit model are calculated for standard test conditions. The five parameters are the light generated current I_L, the diode reverse saturation current I_0, the modified ideality factor a, the series resistance R_s and shunt resistances R_{sh}. The modified ideality factor is a function of the diode ideality factor and number of PV cells within the module (obtained from module data sheet). The authors of this model have also provided a solver to determine the parameters from the module data sheet [40].

The parameters for a commercially available PV module are obtained using the solver and a model of the module is built using the Simscape tool in Simulink (Figure 3.2). The model accepts irradiance and temperature as inputs and outputs the entire I-V curve sweep of the module as shown in Figure 3.1. Additionally, current and voltage

Parameter	**V**alue
Number of cells in series	72
I_{SC} at STC	5.40 A
V_{OC} at STC	44.4 V
I_{MP} at STC	4.95 A
V_{MP} at STC	35.4 V

Table 3.1: Module Data Sheet Ratings

sensors are added to the model to emulate module level monitoring system measurement (Figure 3.3). Modules are connected in series and parallel to form the array. Current and voltage sensors at the end of each string emulate string level monitoring system measurements. In this work, the five parameter model of PV module built in Simulink is used to generate the PV array output data for both faulty and non faulty cases. The module used is Sharp NT-175U1 whose specifications are given in Table 3.1. The module outputs 175 W at standard test conditions.

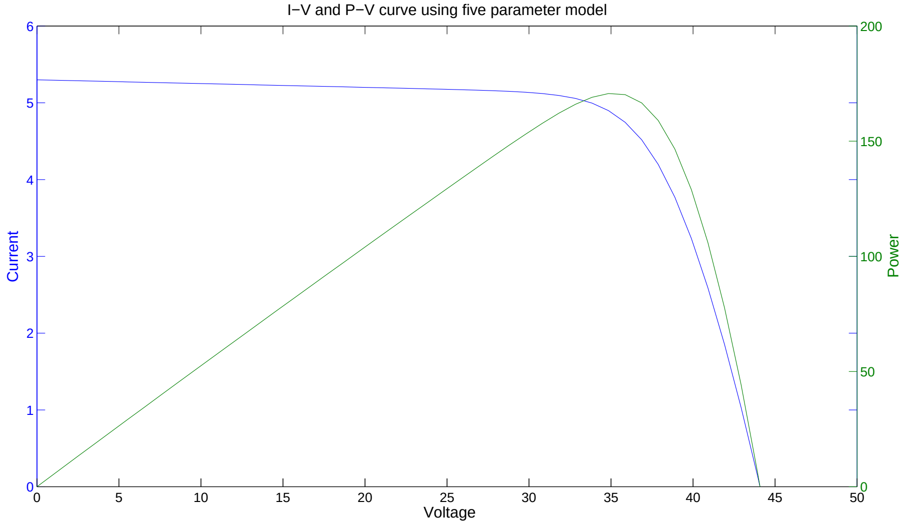

Figure 3.1: I-V, P-V curve of module generated using five parameter model.

Sandia Model

The Sandia model [25] is an empirical model developed by field testing of modules. The Sandia model is a comprehensive performance model incorporating all the factors affecting the solar array. The factors considered in the model include irradiance, back

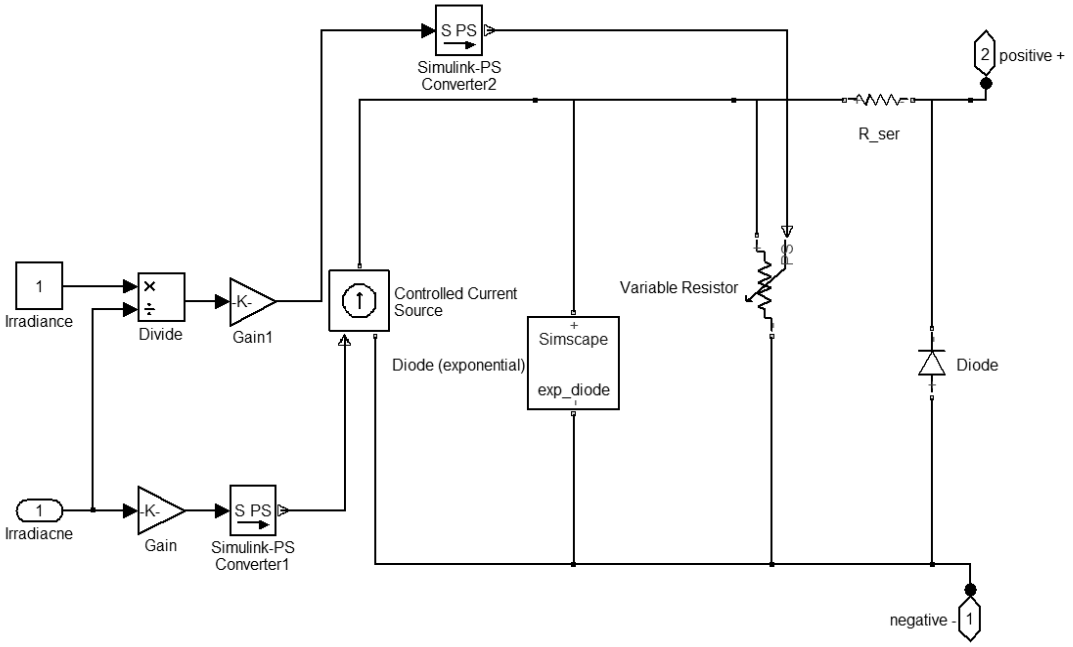

Figure 3.2: Simulink model for PV module.

surface module temperature, wind speed, angle of incidence and air mass. The model is highly accurate and can be used for both flat-plate and concentrator modules. The model provides equations to calculate five points on the I-V curve which can be interpolated to get the entire curve. These include equations to calculate the maximum power point voltage and current, short circuit current, open circuit voltage and two points with voltages halfway between short circuit and V_{MP} and halfway between V_{MP} and open circuit respectively. The equations work well for both individual modules and arrays. The parameters for the equations are obtained by curve fitting methods. A database of parameters are available for many of the commonly available PV modules. The Sandia model for a commercially available PV module implemented in MATLAB is shown in Appendix A. In this work, the Sandia model is used to generate the expected output currents and voltages of the PV array. These are then compared against the outputs generated by the Simulink based circuit model.

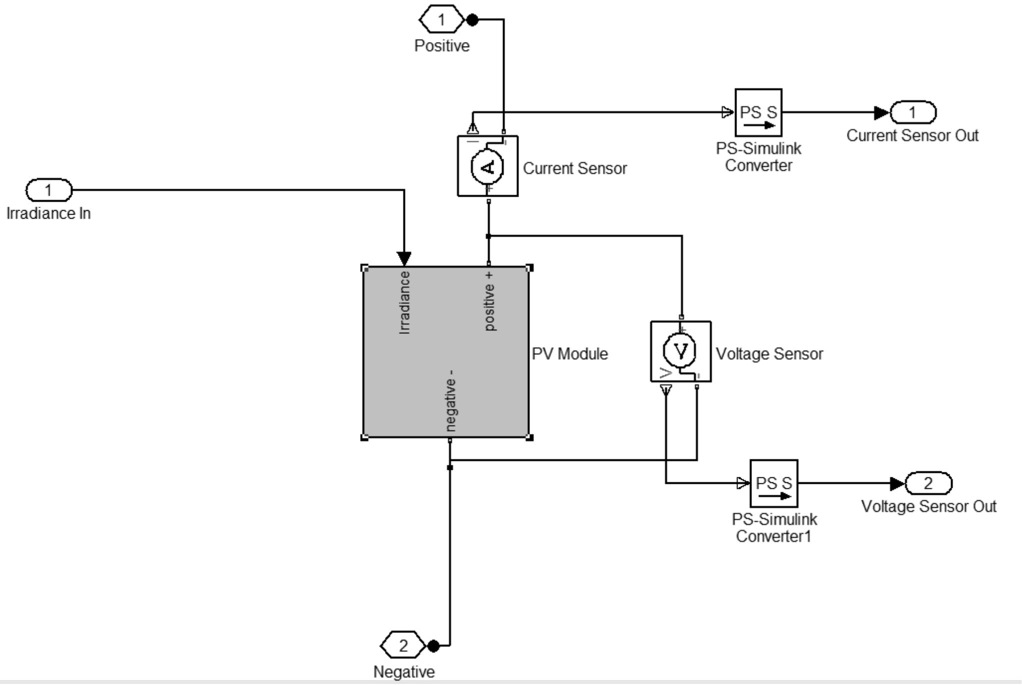

Figure 3.3: Simulink model for PV module with sensors.

Generating PV Array Data

Simulink models are used to generate both faulty and non faulty data. A PV array is built by connecting PV modules in series and parallel. The PV modules with current and voltage sensors shown in Figure 3.3 are used. The array model built in Simulink is shown in Figure 3.4. It consists of 52 modules connected in a 13 series, 4 parallel strings arrangement. The modules accept irradiance and temperature as inputs and output the voltage and current. The currents and voltages output by the modules in each string are multiplexed and stored. Additionally, sensors are added to measure the voltage and current generated by the array and at the end of each string. The array is connected to a reference ground and a solver. The output of the array is connected to a voltage source and the function of the inverter is approximated by doing a full sweep of the voltage and measuring the current. This returns I-V curves for the array, each string and each module. The maximum power point operating voltage and current are determined from the I-V curve of the array.

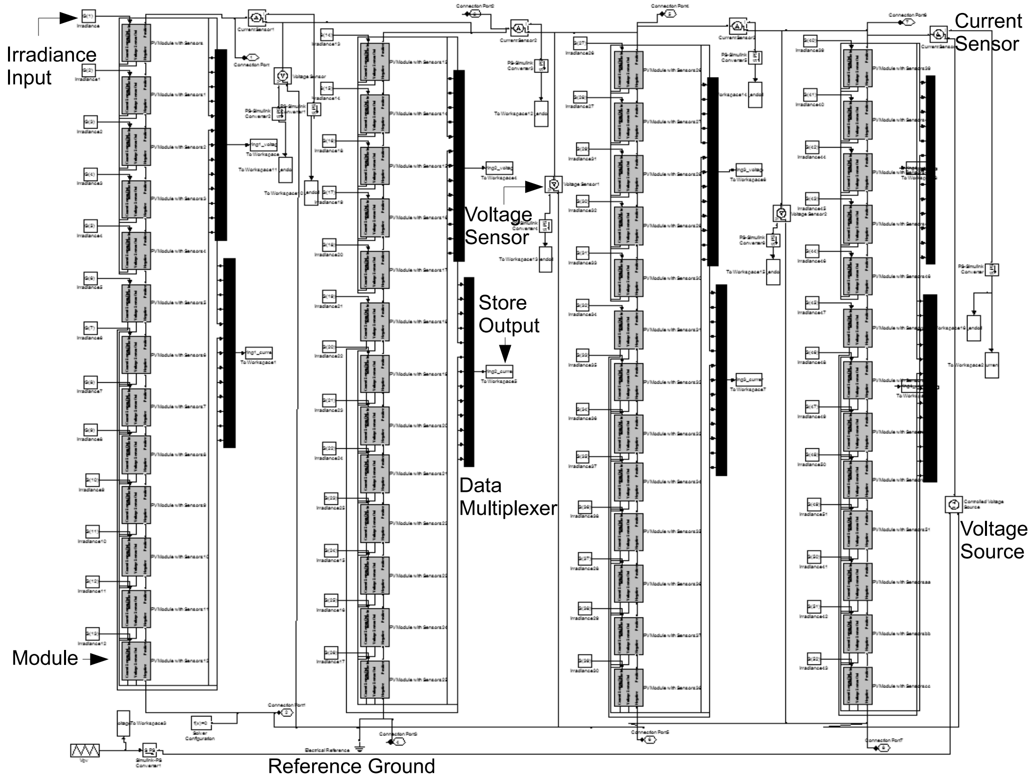

Figure 3.4: Simulink model for 52 module PV array with array, string and module sensing.

Non faulty data is generated by running the model with weather data across the entire day. The array is assumed to be in operation in Tempe, AZ. Irradiance and temperature information is obtained from an experimental monitoring system set-up in Tempe, AZ. The monitoring system measures the values every minute. The non faulty data is generated for an entire day and it corresponds to a wide spectrum of input values.

Faulty data is generated by modifying the PV array model to incorporate faults. Ground faults and shading are considered in this work. Ground fault occurs when there is a low resistance path to the ground. This is modelled in Simulink by connecting a very low resistance between the point of the fault and the reference ground of the circuit. Depending on the location point of the fault, the output of one or more modules are affected. Shading occurs when part or the entire sunlight reaching a PV module is blocked. Shaded module is modelled in Simulink by reducing its irradiance input.

Comparison Metrics

The performance of array, string and module level sensor placement techniques are compared by their ability to detect faults within the array. The data points corresponding to faulty and non faulty array operation are generated using the Simulink model. The output of the Simulink model at the maximum power point is compared against the predicted output of the Sandia model. If the output current, voltage or power differ from the Sandia model expected values by more than a fixed threshold percentage, the data point is classified as faulty. The fault detection probability is compared against the probability of false alarm for each type of fault.

False alarm probability is determined by classifying non faulty data. Monte Carlo simulations are performed by classifying the data points corresponding to non faulty data. The simulations are repeated for various thresholds and the number of data points classified as faulty are obtained. The number of data points classified as faulty divided by the total number of data points classified gives the false alarm probability for that threshold. Fault detection probability is determined by classifying faulty data. Monte Carlo simulations are performed by classifying the data points corresponding to each type of fault for different thresholds. For a given threshold, the number of data points classified as faulty divided by the total number of data points classified gives the detection probability. The thresholds used are the same as those used with the non faulty data. Hence, each detection probability corresponds to a specific false alarm probability rate. Receiver operating characteristics (ROC) curves which plot the detection rate (true positive rate) versus the false positive rate are plotted for each sensor placement technique.

The sensor placement techniques are also compared by plotting the detection rate versus number of the faulty modules for specific false alarm probabilities. The false alarm probabilities considered are 1e-3 and 1e-4 which correspond to 0.1 percent and

0.01 percent respectively. The false alarm probabilities chosen are very high compared to applications in signal processing. However, measurements in PV arrays are typically taken once every minute. This corresponds to about 1 false alarm per average solar day for 1e-3 and 1 false alarm per fortnight for 1e-4 case. In addition to this, the decisions taken are based on average of several measurements. Hence, these false alarm rates are considered. The number of faulty modules corresponds to number of modules affected directly by the fault. For instance, if 5 modules are shaded uniformly, the number of faulty modules is 5 even if the other modules in the string are away from maximum power point due to the effect of shading.

Measurement Errors and Model Mismatch

The measurement errors in sensors and mismatch between simulation data and the Sandia model are modelled as noise. The current and voltage sensors that measure array, string and module output are inaccurate and have noise including quantization noise associated with them. These are modelled as uniform random noise with a distribution of +/- 2 percent corresponding to commercially available sensing devices. Similarly, the irradiance sensors used are inaccurate. In general, lower cost silicon photodiode pyranometers with accuracy of +/- 5 percent are used [41]. This error is modelled as uniform random noise with a distribution of +/- 5 percent. The Sandia model used to predict the expected output of the array differs from experimental output. Studies have been performed to characterize the error associated with the Sandia model [42,43]. For crystalline silicon PV modules, the root mean square (RMS) error of the deviation in current at maximum power point was determined to be between 4.7 and 5.5 percent for the two tested modules [42]. In this work, we consider modelling mismatch to have a 5 percent RMS error. This is modelled in the simulation by an additive Gaussian noise with mean zero and 5 percent variance.

3.3 Results

The PV array is built using 52 sharp NT-175U1 modules in a 13 series 4 parallel configuration. PV array data for non faulty operation is obtained from the array model. The irradiance and temperature values are chosen from an experimental monitoring set-up in Tempe, AZ and cover a wide range of values. Faulty data is obtained by introducing ground fault and shading in the array. Sensor measurement noise of 2 percent uniform noise for current and voltage sensors, 5 percent uniform noise for the irradiance sensor and zero mean, five percent variance Gaussian modelling noise are added. Monte Carlo simulations are performed for faulty and non faulty data for different thresholds and the fault detection rates and false alarm probabilities are obtained for each threshold.

Ground Fault

Ground fault is simulated in a module by connecting the positive terminal of the module to the reference ground through an one ohm resistor. The fault is simulated for standard test conditions and Monte Carlo simulations are performed for different thresholds to get the fault detection probability.

The ROC curves for array, string and module level monitoring systems when a single module is affected by ground fault is shown in Figure 3.5. Module level sensing is able to identify the presence of fault with almost a probability of 1 across the entire range of false positive rates. In fact, the module level sensing only fails to detect the faults at extremely low false alarm rates (<1e-20 for this simulation set-up). String level and array level sensing cannot identify this fault for any reasonable false alarm rate. String level sensing starts detecting faults at high probability when the false alarm rate is around 0.3 which corresponds to three in ten cases of non faulty data being detected as faults. Array level sensing performs even worse and performs well only close to false alarm rates of 0.6 corresponding to 6 in 10 cases of non faulty data being detected as faults. Hence these two sensing techniques are not suited to detect this fault.

The output of the array with the ground fault case is compared to the one without. The faulty array outputs 2.96 percent less power. In the absence of a ground fault interruption device, this fault will remain undetected for a long time in the array and string only sensor configurations.

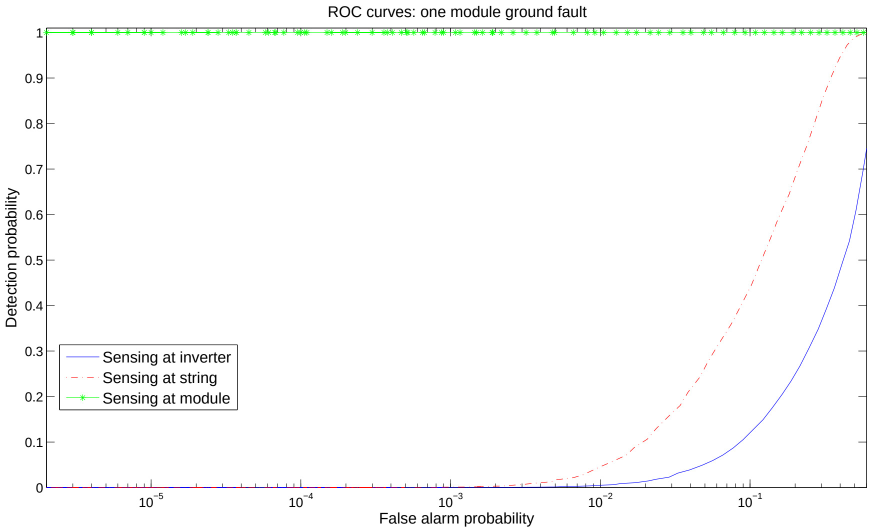

Figure 3.5: ROC curves for array, string and module level measurements : one module ground fault.

The fault detection probabilities for one or more modules affected by ground fault is shown in Figures 3.6 and 3.7. Figure 3.6 plots the fault detection probability when the false alarm rate is 1e-3 (0.1 percent of non faulty data detected as faulty). The module level sensing system is able to detect the presence of fault for even a single module affected by ground fault. The string only measurement cannot detect the case where only one module is faulty. It detects the two modules faulty case with a probability of around 0.35 which is less than the probability of a completely random guess. It can only detect faults consistently for cases where three or more modules are affected. The array level sensing is worse than the string level case and cannot detect faults consistently when less than five modules are affected. Figure 3.7 plots the detection probability for number of modules affected by ground fault when the false alarm probability allowed is reduced to 1e-4 (0.01 percent). Lowering the number of false positives allowed increases the threshold values used to compare the difference in expected and actual values of modules, strings and array. The detector performance for this case cannot exceed the previous case. The performance of the module level detector is similar to the 1e-3 case. However, the string level and array level perform poorly in comparison. The detection probability for string level sensing when three modules are affected drops from 0.98 to 0.82 while the detection probability for four or more modules affected remains mostly the same. Array level sensing can still detect faults when five or more modules are affected, but the detection probability for four modules affected case drops from 0.52 to 0.12. Thus for ground faults, array level sensing is ineffective for faults affecting a small number of modules while string level sensing performs only slightly better.

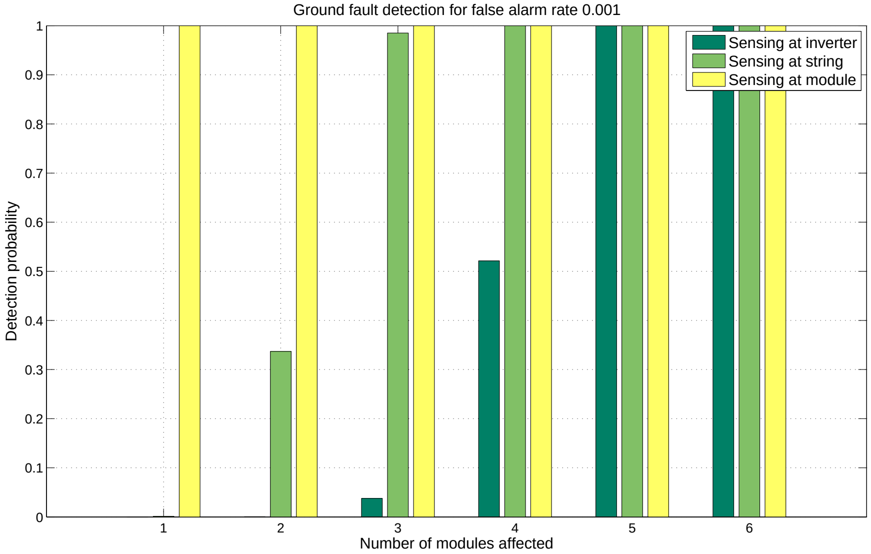

Figure 3.6: Detection probability versus number of modules affected by ground fault : false alarm 1e-3.

Shading

Shading is simulated by reducing the irradiance received by the affected modules while the rest of the modules operate at standard test conditions. The shaded modules receive 5 percent of the incident irradiance. This was chosen to simulate the module being

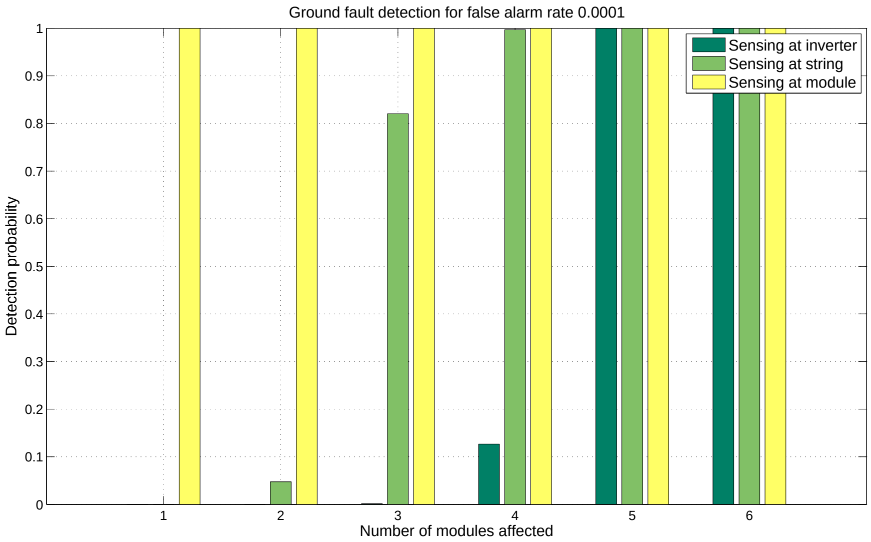

Figure 3.7: Detection probability versus number of modules affected by ground fault : false alarm 1e-4.

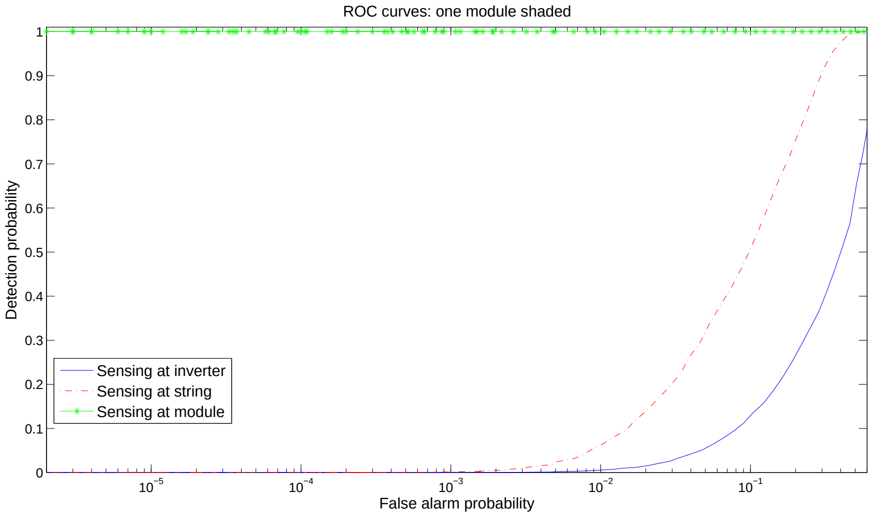

Figure 3.8: ROC curves for array, string and module level measurements : one module fully shaded.

completely shaded while still avoiding numerical errors. Comparisons are done by Monte Carlo simulations for single module shaded, number of modules in the same string shaded and number of modules across several strings shaded cases.

Figure 3.8 shows the ROC curves for the three sensing methods when a single module is shaded in the array. The module is shaded by reducing its input irradiance to 5 percent of actual. The shaded module is bypassed and the remaining modules in the affected string compensate for the reduced voltage. The performance of each sensing method is similar to the ground fault case. Module level sensing has a fault detection probability of almost one except at extremely low false alarm rates. Array and string only sensing is unable to detect the presence of the fault for realistic false alarm rates. String only sensing performs well only for false alarm rates close to 0.2 while array only sensing is worse. This fault corresponds to a 3.2 percent loss of power in the array and cannot be detected by array and string level sensing methods. This is because the uncertainty in modelling and errors in irradiance sensor measurements will lead to unacceptable number of false alarms for a 3.2 percent threshold.

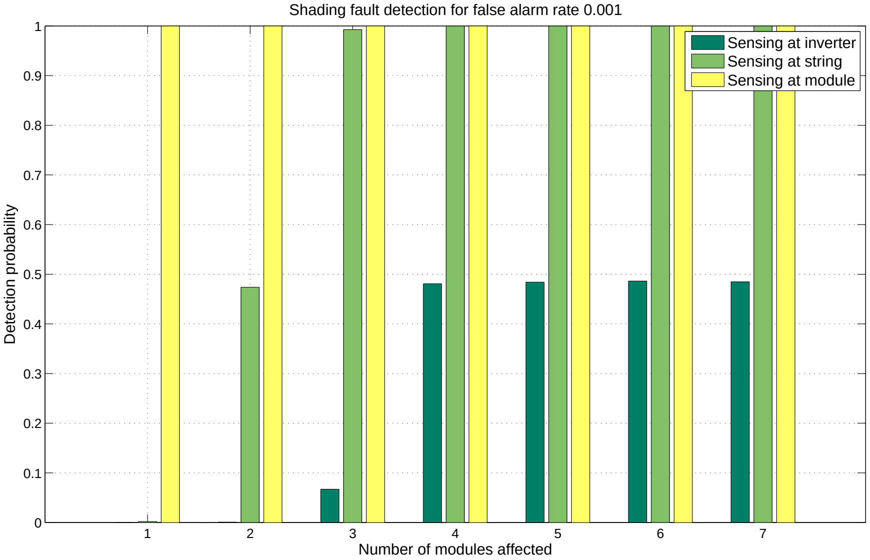

Figure 3.9: Detection probability versus number of modules affected by shading in same row: false alarm 1e-3.

The effect of number of modules affected by shading on the probability of detection when modules in the same row are shaded is shown in Figures 3.9 and 3.10. Figure 3.9 shows the fault detection probability for the three sensing cases when the

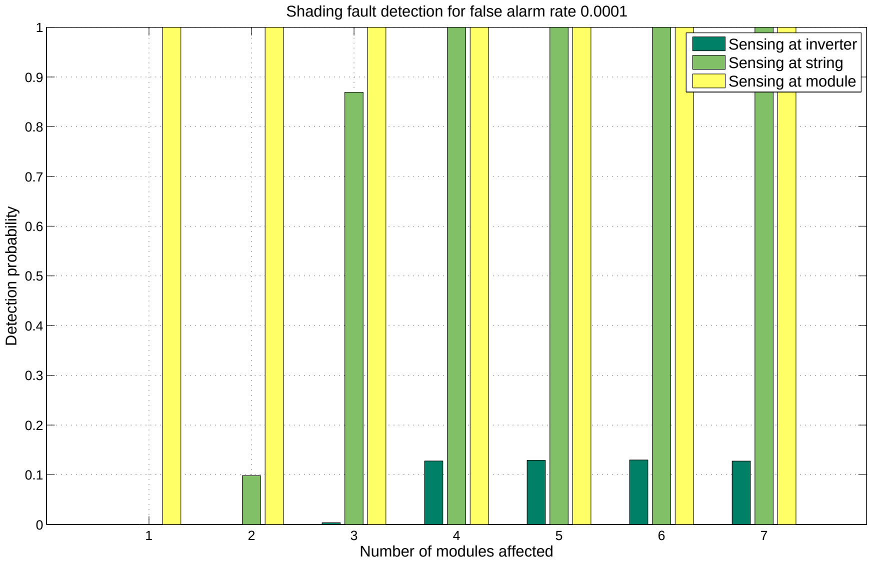

Figure 3.10: Detection probability versus number of modules affected by shading in same row: false alarm 1e-4.

false alarm probability is 1e-3. Module level sensing detects the faults for all the cases including the case where only one module is shaded. String level sensing cannot detect the fault when only one module is shaded. For the two module shaded case, string level sensing has a detection probability of less than 0.5. It can detect faults consistently only when three or more modules are shaded. Array level sensing cannot detect faults consistently even for the case of 7 modules being shaded. Figure 3.10 shows the fault detection probability for the three sensing cases when the false alarm rate is 1e-4. The results for the module level sensing are similar to the 1e-3 false alarm rate case while the detection rates for the string and array level are reduced. The probability of detection for string level sensing drops from 0.99 to 0.87 for three of the modules shaded while detection rates for four or more modules shaded remains unchanged. Detection probability for array only sensing drops for the four or more modules shaded case from 0.48 to 0.12. The detection probability for array level sensing remains the same for four to seven modules shaded. This is because the loss of power due to the effect of the fault becomes maximum when four modules are affected and stays the same even when additional modules are shaded. From the results, it is seen that shading occurring along the same row cannot be detected irrespective of the number of modules affected for array only sensing systems while string level sensing detects faults when three or more modules are affected.

The effect of number of modules affected by shading across rows on the probability of fault detection is shown in Figure 3.11 and 3.12. The shading is done across rows. This means that for number of modules shaded being 4, one module is shaded in each string and for number of modules shaded being 7, three strings have two modules each shaded and one string has one module shaded. Figure 3.11 shows the plot when the false alarm rate for the array is fixed at 1e-3. Module level sensor placement detects the faults with a probability of one. String and array level sensing are very poor in detecting the presence of faults. String level detects faults with probability of approximately 0.7 when the number of modules shaded becomes 9 and cannot detect for cases where lesser number of modules are shaded. Similarly, array level sensing detects faults only when the number of modules affected by shade becomes 13 and more. The detection probability for 12 modules shaded is only 0.18. Figure 3.12 shows the plot when the false alarm rate is 1e-4. Module level sensor placement detects the faults with a probability of one. The detection probabilities of string and array level sensing are reduced. For this case, string level detection performs well only when 13 or more modules are affected while array level cannot detect with high accuracy even when 16 modules are shaded.

3.4 Analysis of Results

This section analyzes the simulation results of the different sensor placement methods. The results of the simulations performed are tabulated. The fault detection capability of each type of sensor arrangement is compared against the loss of power in the array for different fault cases. In this analysis, a good detector is assumed to have detection probability of at-least 0.9.

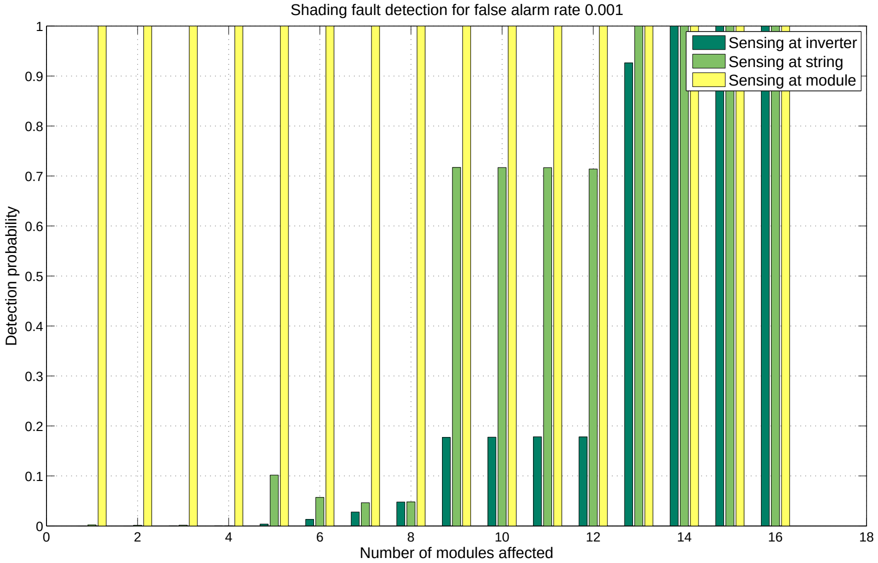

Figure 3.11: Detection probability versus number of modules affected by shading across rows: false alarm 1e-3.

Table 3.2 shows the fault detection probability for the case where false alarm probability is fixed at 1e-3. The fault detector that uses module level sensors performs like an ideal detector with a probability of one for all fault cases. The performance of the string and array level detectors varies depending on the fault type and number of modules affected. String level sensing cannot detect ground faults and shading faults in the same row that affect only two modules. This corresponds to a loss of 8.4 and 9.2 percent power from the array going undetected. For modules shaded across several rows, string level sensing cannot detect faults even when 10 modules are shaded and the power loss in the array is 19.75 percent. Similarly array level sensing performs poorly on ground faults and shading faults that cause up to 23 percent loss of power in the array.

Table 3.3 shows the fault detection probability for the case where false alarm probability is fixed at 1e-4. Since the false positives allowed is reduced, the thresholds for fault detection increase. This results in inferior fault detection performance compared to the previous case for the string and array level sensing. The fault detector

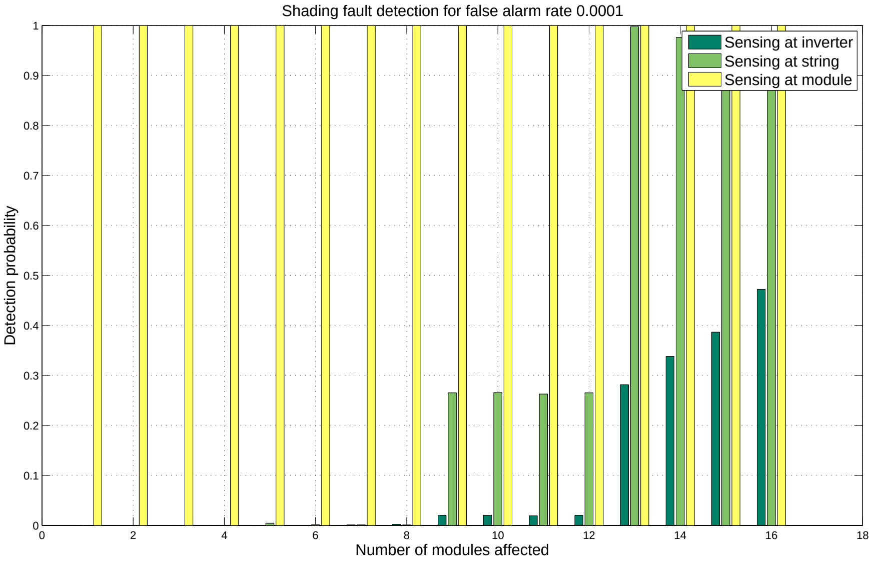

Figure 3.12: Detection probability versus number of modules affected by shading across rows: false alarm 1e-4.

that uses module level sensors still performs like an ideal detector with a probability of one for all fault cases. However, string level sensors cannot detect ground faults that result in loss of 8.4 percent power and shading faults that result in loss of 19.75 percent power with 0.9 probability. Similarly, array level sensing performs poorly on ground faults that cause 23.7 percent loss in array power and shading faults that cause 28 percent loss.

It is clear form these simulations that the array level sensing cannot identify most of the faults within the array even when the loss of power due to the fault is well above 20 percent. Hence we need to include higher resolution sensing for PV arrays. The two potential candidates string and module level sensing can detect faults better than array only sensing. However, string level sensing performs poorly for several cases where there is shading across rows resulting in almost 20 percent loss of power. This is not the case with module level sensing as it detects faults affecting even a single module. Hence module level sensing must be considered where ever possible.

Fault type	**M**odules affected	**P**ercentage loss in Power	**A**rray detection probability	**S**tring detection probability	**M**odule detection probability
Ground	1	2.97	0.0001	0.0011	1
	2	8.43	0.0004	0.33	1
	3	15.74	0.03	0.985	1
	4	23.78	0.52	1	1
	5	32.02	1	1	1
Shading same row	1	3.28	0.0002	0.0019	1
	2	9.27	0.0008	0.47	1
	3	17.05	0.067	0.99	1
	4	23.66	0.48	1	1
	5	23.67	0.48	1	1
Shading across rows	2	5.4	0.0002	0.001	1
	4	8.12	0.0004	0.0004	1
	6	13.62	0.013	0.057	1
	8	16.24	0.048	0.048	1
	10	19.75	0.178	0.717	1
	13	26.25	0.926	1	1
	16	28.01	1	1	1

Table 3.2: Fault detection probability compared to loss of power in array for false alarm probability of 1e-3.

The poor performance of the string level and array level sensing is mainly due to the uncertainty in the models used to predict the output power and in measuring irradiance. Using a higher quality irradiance sensor or obtaining better irradiance data from weather databases and time averaging the expected and actual array outputs would improve the detection rates for these cases. However, most faults that affect only one or two modules in the array will still go undetected.

Module level sensing has a fault detection probability of 1 for all the cases. This is because the length of the Monte Carlo runs chosen were not sufficient to allow the detector to fail. Repeating the simulations for higher length runs would result in the probability of detection dropping to less than one. Since such high precision is not necessary to compare the performance of different configurations, it was not considered.

Fault type	**M**odules affected	**P**ercentage loss in Power	**A**rray detection probability	**S**tring detection probability	**M**odule detection probability
Ground	1	2.97	0	0.00005	1
	2	8.43	0	0.047	1
	3	15.74	0.0014	0.82	1
	4	23.78	0.127	0.997	1
	5	32.02	1	1	1
Shading same row	1	3.28	0	0.00004	1
	2	9.27	0	0.098	1
	3	17.05	0.003	0.87	1
	4	23.66	0.12	1	1
	5	23.67	0.12	1	1
Shading across rows	2	5.4	0	0	1
	4	8.12	0	0	1
	6	13.62	0.0003	0.001	1
	8	16.24	0.0019	0.001	1
	10	19.75	0.02	0.267	1
	13	26.25	0.28	0.99	1
	16	28.01	0.47	0.91	1

Table 3.3: Fault detection probability compared to loss of power in array for false alarm probability of 1e-4.

3.5 DC Monitoring System Overheads

Though the DC monitoring system improves fault detection capability of the PV array, it comes with additional costs related to data gathering, storage and processing. This section talks about the costs involved with setting up a DC monitoring system. These are based on ‘off the shelf’ commercially available resources and may not reflect accurately the costs for a dedicated PV monitoring system.

- Data gathering. This consists of sensors that measure the data and communication systems that transmit the data. Currents and voltage sensors are commercially available for less than ten dollars. Communication channels to transfer this information to the central server are more expensive. Transceivers that can communicate with one another and send the sensed values to the server can cost anywhere between 25 and 100 dollars

- Data processing. Since only minute by minute data is stored, the processing power required from the central server is less. Hence commercially available servers that cost a few hundred dollars can handle multiple arrays. However the energy cost involved in running the server for the entire year need to be considered

- Data storage. The cost of data storage is decreasing. Recent cloud based storage services provide a gigabyte of data storage for about 10 cents. At this rate, storing minute by minute data from all the modules within the array for an entire year would cost only a few dollars

- Software. The cost of software that integrates the data processing algorithms with displays must also be considered

Apart from software costs the rest of the requirements of a DC side PV monitoring system can be estimated approximately using equivalent commercially available systems. The cost of storage and servers are very less. Even the transceivers cost less compared to the price of modules and inverters. Hence it might be good practice to incorporate DC monitoring in all new PV arrays.

3.6 Summary

This chapter compared the performance of array, string and module level monitoring systems in detecting ground and shading faults. Module level monitoring system had the best performance and was able to detect faults with a probability of almost one. String level monitoring systems cannot detect shading and ground faults that affects one or two modules. Array level monitoring is unable to detect ground faults that affects up to four modules and shading that affect five modules in the same row. From the simulations it is clear that many of the potential faults in current arrays go undetected. String level sensors are able to detect most of the faults that affect more than two modules and must be considered essential for PV arrays. Module level measurements must be considered in cases where the loss of power from even one or two modules is considered unacceptable.

Chapter 4

DEMONSTRATION GRAPHICAL USER INTERFACE

This chapter describes a demonstration GUI built in MATLAB, utilizing data obtained from an experimental monitoring system in Tempe, AZ. This GUI is used to discuss some of the user interface features for the monitored data and algorithms that a module level monitoring system GUI can have.

Automated PV monitoring generates a lot of information about the state of the array. This may include power output by the array, DC currents and voltages at the inverter input, current and voltage outputs of modules and strings and weather data. The monitoring systems can collect this data several hundreds of times in a day. They can use different data acquisition systems to collect inverter and module/ string data. Weather data might be obtained from a weather station installed at the PV site or from a national weather database. The array owner/ operator requires proper tools to process this data from different sources and make sense of it.

PV array monitoring GUIs can have a wide range of tools depending on the data available to them. GUIs with access to weather information can integrate PV models and compare expected output and actual output. GUIs with access to historical output of the array can display monthly or yearly yield information. Output for a month can be compared to the output for the same month from a previous year to calculate the efficiency of operation of the array. Data for the year can be compared to previous years to calculate the annual de-rate factor. Data from the array can be used in signal processing algorithms to detect the presence and location of faults within the array.

These tools must present the information in a easily understandable form. For instance, the expected output can be plotted along side the actual output as a bar graph. For arrays that monitor at module and string level, the GUI must present the information about the array without overwhelming the user. Displays for array level, string level and module level output must be separated and the user must be provided with means to navigate between them. The GUI must be simple and easy to use. The visualizations must convey the health of the array without the need for the user to have much technical knowledge. Hence GUIs must integrate the tools with insightful data displays.

A demonstration GUI is built that accepts module level information from a PV array. The main motivations for building the demonstration GUI are to integrate signal processing algorithms for fault detection and PV models developed in a single easy to use software and test different data visualizations for module and array level data. The demonstration GUI concentrates on the DC side monitoring of PV arrays.

4.1 Demonstration GUI Overview

The demonstration GUI is built in MATLAB. Weather, module and array data are integrated with Sandia model and a fault detection algorithm. Real time updates of module level and array level information is provided to the user.

GUI Development Tool

The GUI is built using MATLAB. MATLAB contains several signal processing libraries and other vector manipulation functions making it easier to develop PV array models and fault detection algorithms. It provides tools to build GUIs either through command line or graphical placement. The developed GUI can be integrated with other algorithms and output displays built in MATLAB. There are tools to compile the MATLAB GUI as an external standalone application if required. Hence MATLAB was chosen to build the demonstration GUI.

Monitoring Data Available to GUI

Weather, module data and inverter data is available to the GUI from an experimental set-up on an array of 52 modules. Irradiance, atmospheric temperature and wind speed are collected by a weather station installed at the site every minute and stored along with the time stamp. Data acquisition system collects the voltage and current from the

DC and AC side of the inverter every minute. Similarly, monitoring devices installed at the back of each module collects the voltage, current and back of module temperature every minute.

The different monitoring systems store the data collected in different formats. Additionally, the module level information contains communication protocol information such as handshake signals. Scripts written in ‘Perl’ process the module data and convert them in to vectors with just current, voltage, temperature and time information. ‘Perl’ is chosen since MATLAB provides support for calling Perl script files from MATLAB functions. Scripts are used to combine the outputs of different data acquisition systems and align the data according to time stamp.

Fault Detection Algorithm

The GUI has access to module level voltage and current information for each time instance. This information can be used to detect faults within the array. The expected outputs of the modules can be calculated from weather data. The percentage difference between the expected and actual output voltage and current can be compared to a threshold to detect the presence of faults. However, identifying the exact location of the fault presents some challenges. This is because, the faulty module affects other modules in the string and simple threshold based comparisons might detect multiple modules as faulty. For instance, consider the case where a single module in the array is affected by ground fault as shown in Figure 4.1. The faulty module operates close to the short circuit. The rest of the modules in the string compensate for the reduced voltage by operating away from their maximum power points. Normal threshold based algorithms cannot distinguish the two cases. Hence we need sophisticated signal processing algorithms to determine the faulty module. Fault detection is performed using the minimum covariance determinant (MCD) algorithm. MCD is a robust-statistics based algorithm that can identify an outlier in the presence of multiple clusters. The MCD algorithm has been shown to be effective for detecting PV array faults [28].

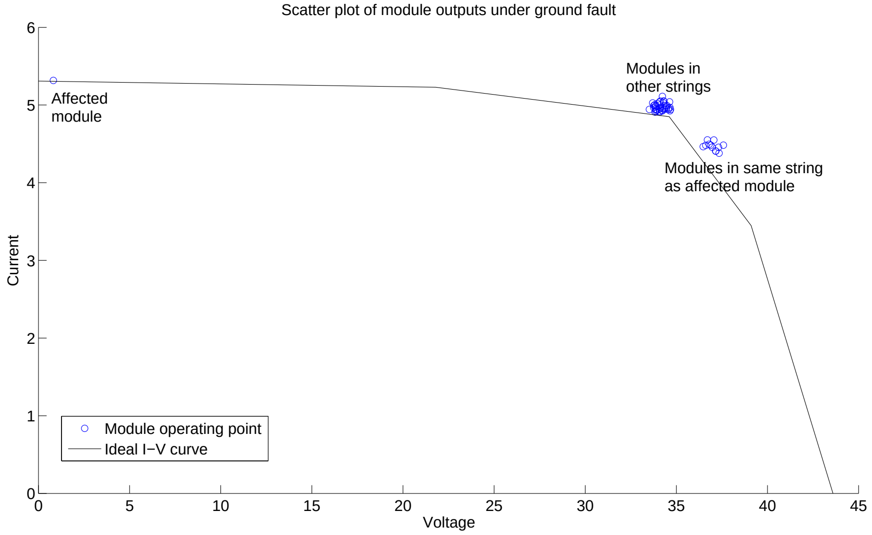

Figure 4.1: Operating points of modules in the array when one module is affected by ground fault.

4.2 GUI Control Flow

The GUI consists of several components such as buttons, plot axes, lists and text boxes. These display information about the array and provide navigation control and plot options. Additionally the GUI updates its displays based on timer events and user action. The GUI is designed with a control flow to create GUI elements, read and display array data and react to user events.

The control flow for the demonstration GUI is shown in Figure 4.2. The overall figure is created with components for the different tabs, buttons and display axes. Tabs are created by creating panels for all the tabs on top of each other and controlling the visibility based on the selected tab. Callback functions are assigned for the buttons and timer updates. Callback functions are instructions that need to be executed when a specific event occurs such as a button press by the user.

The data is read from the monitoring system. The inverter, module and weather data can be from different sources. The data from the different sources are parsed, time

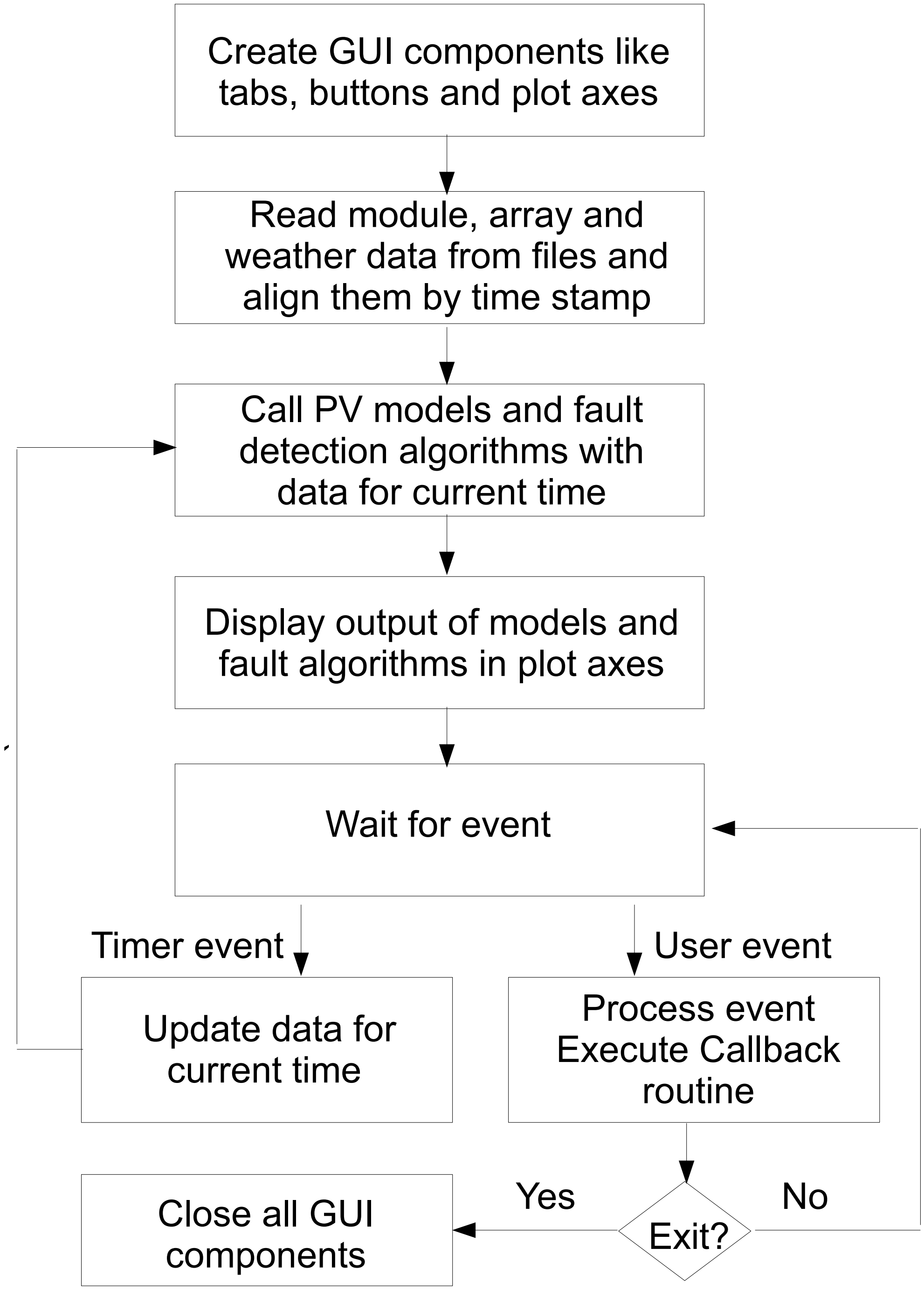
Create GUI components like tabs, buttons and plot axes
Read module, array and weather data from files and align them by time stamp
Call PV models and fault detection algorithms with data for current time
Display output of models and fault algorithms in plot axes
Wait for event
Timer event
User event
Update data for current time
Process event Execute Callback routine
Yes
No
Exit?
Close all GUI components

Figure 4.2: Control flow to create and execute the visualizations for the GUI.

aligned and made in to a single usable data structure. The irradiance and temperature values obtained from the weather data are used in the Sandia PV model to calculate the expected output for the array and individual modules. The module level current and voltage monitoring information is used as input to the MCD algorithm to detect faults. The data obtained from the monitoring system, PV models and fault detection algorithm are displayed in the axes created.

Once the GUI has executed all the scheduled tasks it waits for events to occur. Once a event is detected, the GUI calls the appropriate callback routine. The GUI executes the given list of tasks in the callback routine and returns back to the wait state. Two types of events occur in the demonstration GUI. The first kind is called a timer event and it occurs once every minute. For a timer event, the GUI reads the PV array information corresponding to the current time. It calculates expected PV output, detects faults for the current set of values and updates the displays. The second type of event is the user initiated event. This occurs when the user presses a button or changes the display. In this case, the GUI executes the callback routine corresponding to the button pressed. If the button pressed is the terminate button, the GUI shuts down.

4.3 GUI Features

The GUI has algorithms that predict the expected output and detects faults. It also has displays that provide information about the site, array and module. These different features are organized in the GUI by means of tabs. The different tabs in the GUI are

- Array summary : contains visualizations for the output of the entire array
- Array map: provides a visual representation of the physical arrangement of modules
- Module data: contains visualizations for each module in the array
- Fault detection: provides a visual representation for the MCD fault detection algorithm

In addition to these tabs, the GUI also displays site, weather and time information and predicted array output values. This section describes the control flow used in designing the GUI, the basic structure of the GUI and the functionality of each tab.

GUI Structure

The GUI is separated into three segments displaying site summary information, tab selection and data display. The start-up screen of the demonstration GUI is shown in Figure 4.3. The top panel shows the summary information for the site and is always visible. This panel contains the site location information, instantaneous power output by the array and expected power output by the array. The actual power output is obtained from the inverter data acquisition system and expected power output is calculated from the Sandia model. The outputs displayed are updated every minute. The current weather condition is indicated using a graphic which corresponds to irradiance, temperature and cloud conditions. In Figure 4.3, a sunny graphic corresponding to irradiance of almost 1000 W/m^2 is shown. The left panel displays the local time and tab buttons to switch between the different visualizations. The tab buttons correspond to displays for summary, module data, fault detection and module location information. The current tab selection is highlighted and shown in white. The right panel is used to displays the plots for each the selected tabs. The content in the right panel changes when switching from one tab to another.

Array Summary

The array summary tab can display the power output by the array across each time instant in the day or across several days and compare it to irradiance. It can display hourly average or daily average power output by the array and compare it to expected values. It also displays the total and average power output for the current day. The summary tab has different visualization plots which can be selected by clicking on the buttons available on top of the plot. The different visualization in the summary tab are

- Irradiance and output power across time for current day
- Irradiance and output power across time for a date and time range

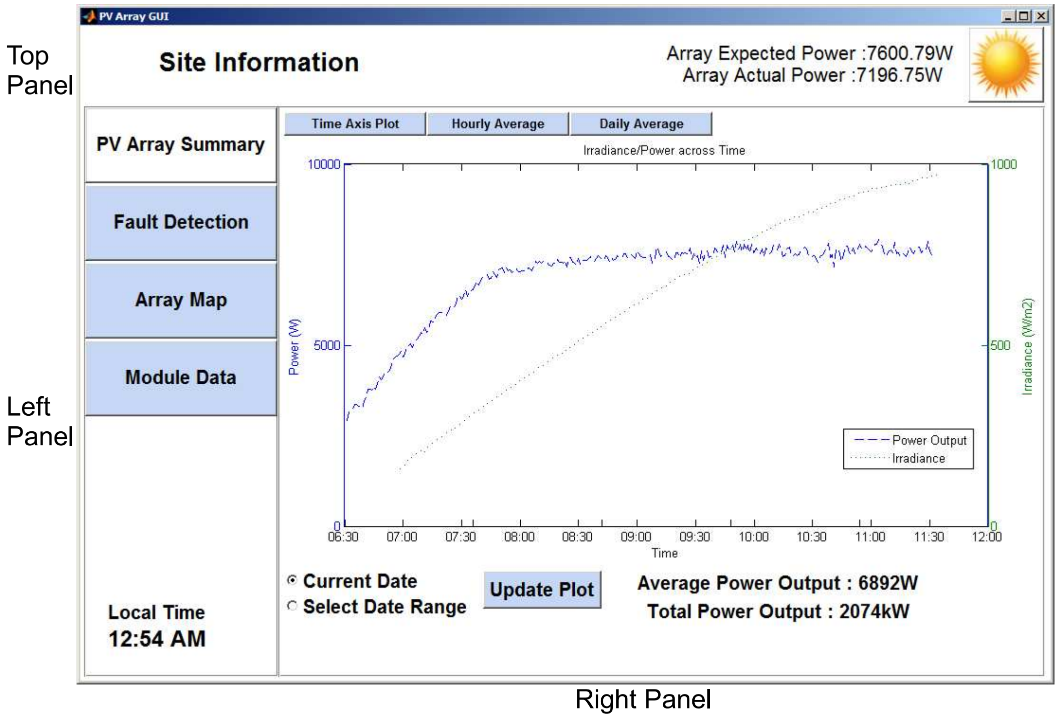

Array Expected Power :7600.79W
Array Actual Power :7196.75W

Average Power Output : 6892W
Total Power Output : 2074kW

Local Time
12:54 AM

Figure 4.3: Structure of PV monitoring demonstration GUI.

- Hourly average of expected power and actual power for current day
- Hourly average of expected power and actual power for a date and time range
- Daily average of expected power and actual power

The default display of the summary tab is shown in Figure 4.3. It plots the output power and incoming irradiance across time for the current day. The 'x axis' plots the time across the entire day. The power output by the array in Watts is plotted on the 'y axis' in blue with a dashed line. The irradiance in W/m^2 is plotted on the 'y axis' in green with a dotted line. Data points are considered for every minute of the day. The output power of a solar array largely depends on the irradiance received. Hence this summary plot can provide a visual representation of the efficiency of operation of the array. Low power output for high irradiance values can alert the operator to catastrophic faults in the array.

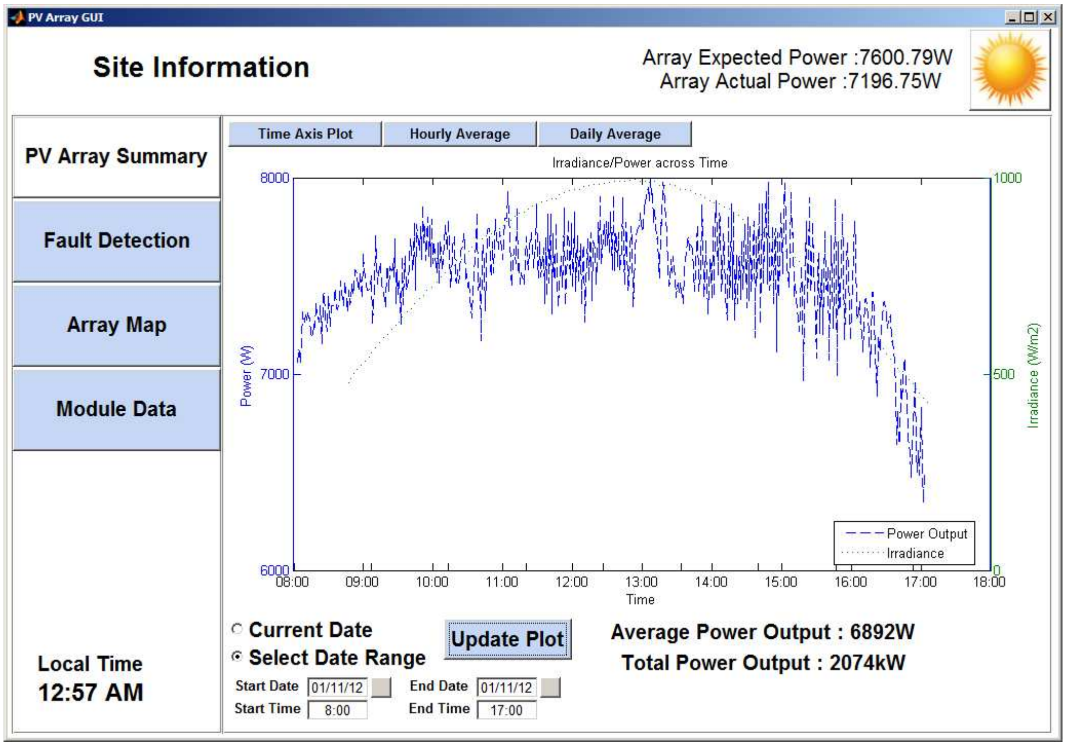

Array Expected Power :7600.79W
Array Actual Power :7196.75W

○ Current Date
● Select Date Range

Start Date 01/11/12
Start Time 8:00
End Date 01/11/12
End Time 17:00

Average Power Output : 6892W
Total Power Output : 2074kW

Local Time
12:57 AM

Figure 4.4: PV GUI : array power output and irradiance across time for a selected date range.

The summary information can be plotted for the current date or for a specific date and time range using the radio buttons present below the plot. Selecting a date range displays text boxes to the enter start date, start time, end date and end time as shown in Figure 4.4. Users can either enter the date manually or through a pop up calender that appears when they click on the buttons next to the start and end date text boxes. Once the date and time range is selected, clicking the update plot button changes the plot. In Figure 4.4, the data for one day is plotted from 8 AM to 5 PM. The user can get back to the current date by selecting the current date radio button and updating the plot.

The summary tab plot can be changed to display hourly averages for the current day or a range of days by selecting the 'Hourly Average' button on top of the plot. Figure 4.5 shows the GUI when the hourly average button is selected. The 'x axis' displays the time across the day in hourly intervals. The average expected power and

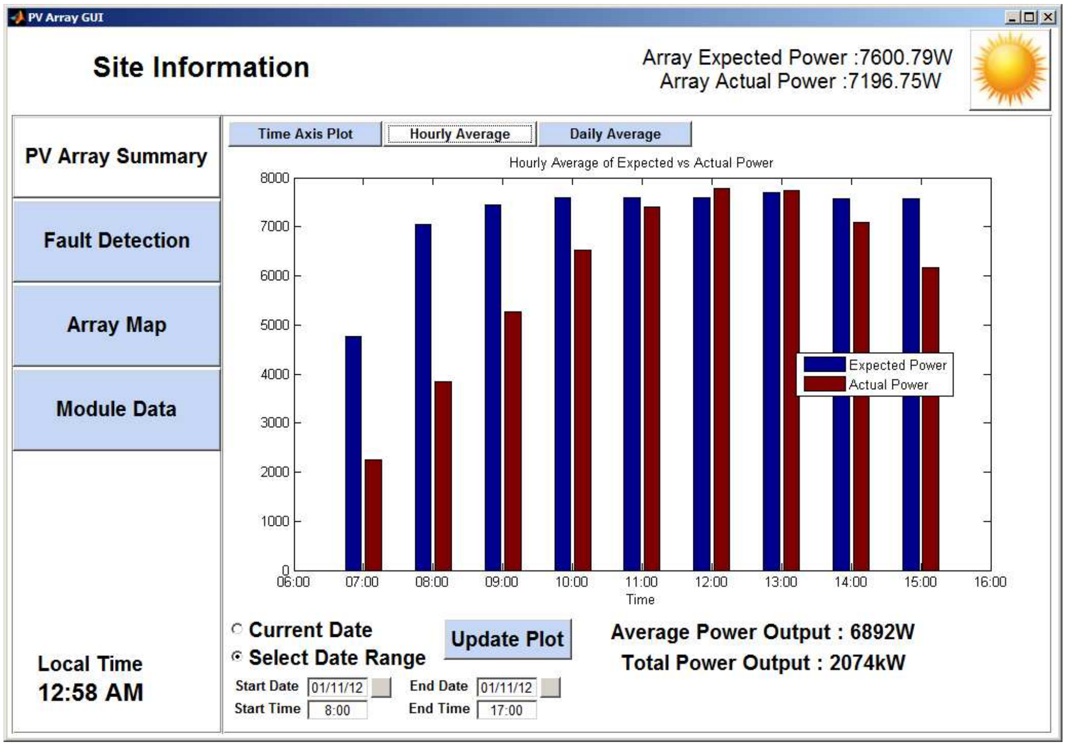

Site Information

Array Expected Power :7600.79W
Array Actual Power :7196.75W

○ Current Date
● Select Date Range

Start Date 01/11/12 End Date 01/11/12
Start Time 8:00 End Time 17:00

Average Power Output : 6892W
Total Power Output : 2074kW

Local Time
12:58 AM

Figure 4.5: PV GUI : hourly averages of expected and actual power.

actual power are plotted on the ‘y axis’ in the form of bar graph. This display can be used to identify the performance of the array over specific time periods in the day. For instance, if the array gets shaded only during evening hours, the actual power would be much less than the expected power during that period.

The summary tab plot can be changed to display daily averages by clicking on the ‘Daily Average’ button on the top of the plot. Figure 4.6 shows the GUI when the daily average button is selected. The ‘x axis’ displays the day with each data point representing one day. The ‘y axis’ plots the average expected power and average actual power across each day in the form of bar graph. Similar displays can be added for weekly or monthly plots.

Array Map

The array map provides a graphical representation of the physical location of each module within the array. It helps the user identify the location of the faulty module

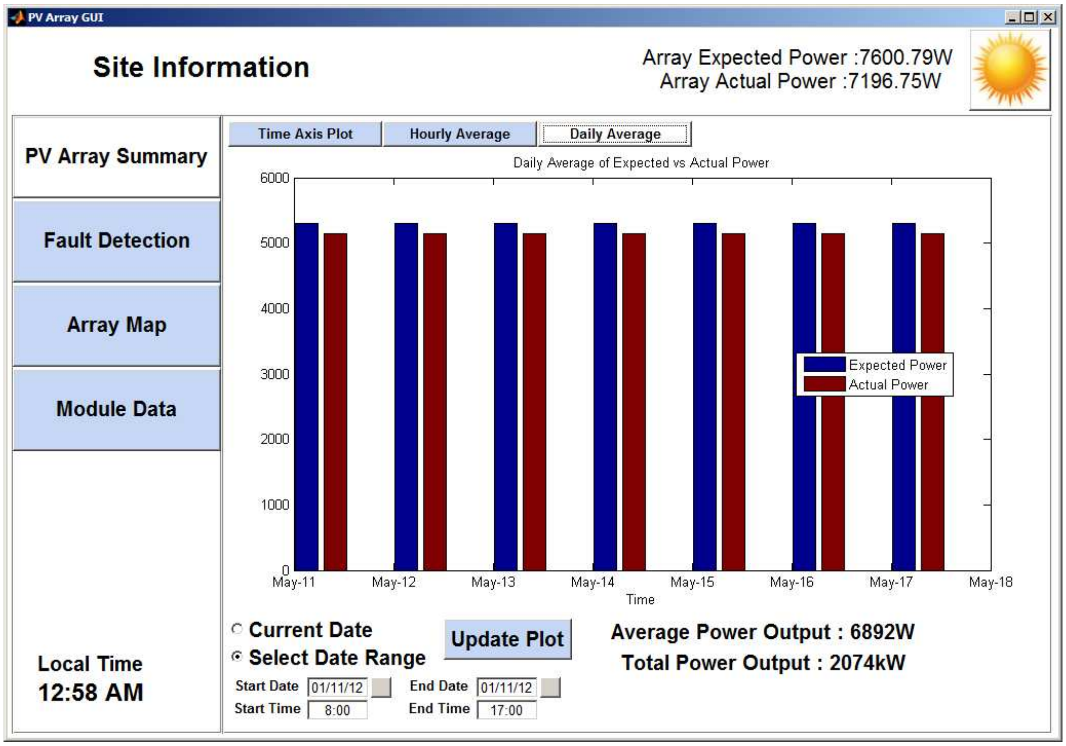

Array Expected Power :7600.79W
Array Actual Power :7196.75W

Local Time
12:58 AM

○ Current Date
● Select Date Range

Start Date 01/11/12
Start Time 8:00
End Date 01/11/12
End Time 17:00

Average Power Output : 6892W
Total Power Output : 2074kW

Figure 4.6: PV GUI : daily averages of expected and actual power.

determined by fault detection algorithms and display the instantaneous power output by each module.

Figure 4.7 shows the array map display for a 52 module array. Each module is displayed as a button with a number from 1 through 52. As the map indicates, the array is configured in a 13 series, 4 parallel arrangement. Any module in the array can be selected by clicking on the corresponding button on the map. The selected module gets highlighted and is shown in white. The instantaneous output by the module is shown below the array along with the expected power. The instantaneous output for the module is obtained from the module data acquisition system and the expected output is calculated from the irradiance and temperature values using the Sandia model. This display is updated with newer information obtained from the array every minute. Figure 4.7 shows the case where module 18 is selected from the map. The instantaneous and expected output power of module 18 is displayed for the current local time. Clicking on the 'Plot Module Data' button changes the selected tab to 'Module Data' tab and

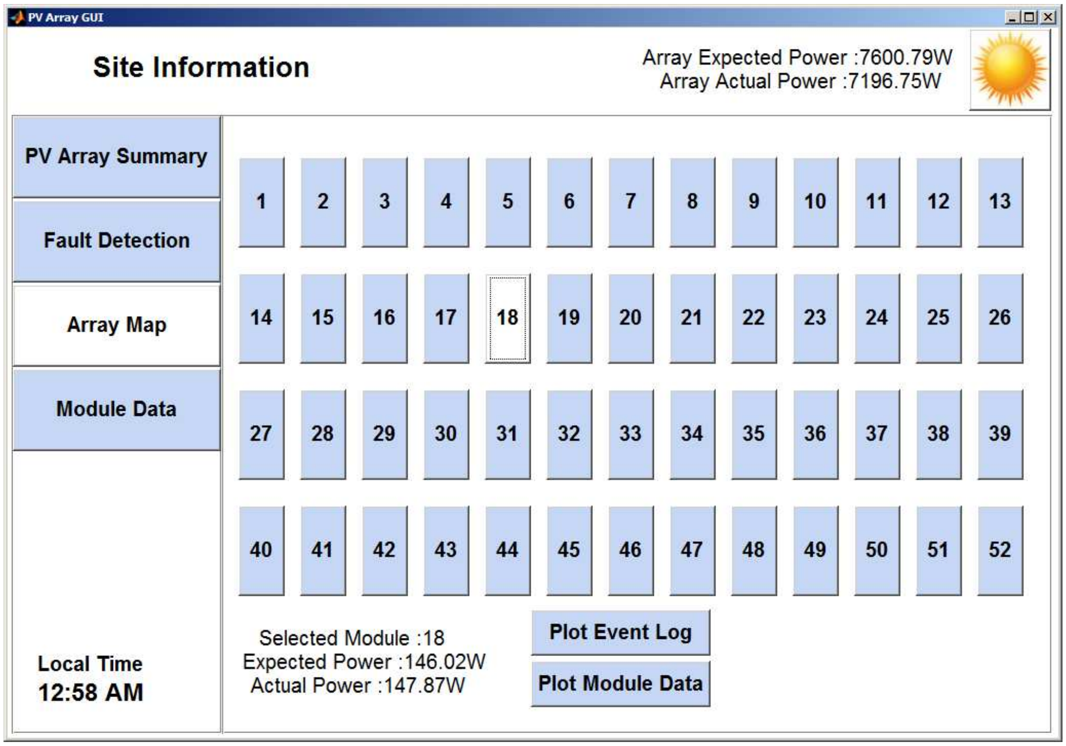

Array Expected Power :7600.79W
Array Actual Power :7196.75W

Local Time
12:58 AM

Selected Module :18
Expected Power :146.02W
Actual Power :147.87W

Figure 4.7: PV GUI: map of modules within the array.

plots the power output across time for that specific module. Similarly the ‘Plot Event Log’ tab transfers the control to the ‘Fault Detection’ tab.

Module Data

The module data tab provides visualization for the output of each module. The output can be for the current day or for a range of dates and time. The expected output power is compared against the actual output power for the specified module.

Figure 4.8 shows the expected and actual power output for module 16. The ‘x axis’ represents the time axis. The expected output power of the module in Watts is plotted in the ‘y axis’ in blue. The actual power is plotted in red. A list box displayed below the plot allows the user to select the module to be plotted. Similar to the array summary tab, the user can plot the data either for the current day or across several days by specifying a range of dates.

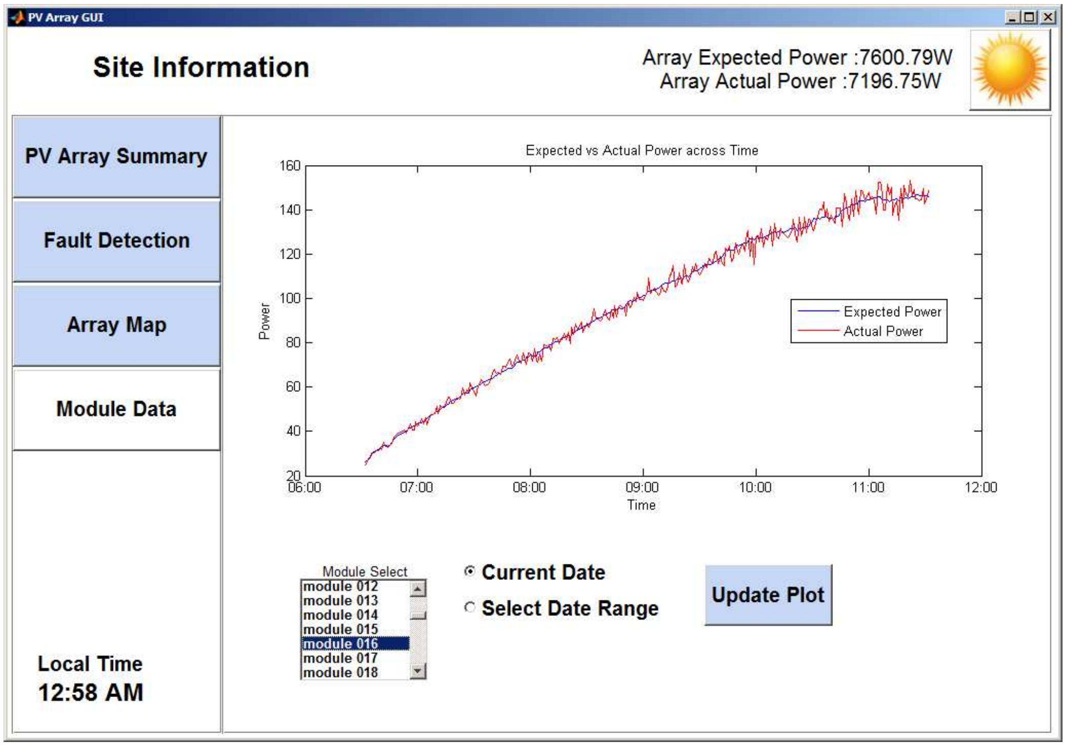

Array Expected Power :7600.79W
Array Actual Power :7196.75W

Module Select
module 012
module 013
module 014
module 015
module 016
module 017
module 018

● Current Date
○ Select Date Range

Local Time
12:58 AM

Figure 4.8: PV GUI: module expected versus actual power.

Fault Detection

The fault detection tab runs the minimum covariance determinant (MCD) algorithm to detect outliers as faults and provides information about the history of events that occurred. The scatter plot of the module output voltages and currents are plotted against the ideal I-V curve and the outlier module is plotted in a different color.

Figure 4.9 shows the output of the GUI for a single faulty module within the array. The ideal I-V curve plot of the module is calculated from the obtained weather data using the Sandia model. Faults are detected as outliers using the MCD algorithm. The non faulty modules are shown in blue and the faulty module is shown in red. Clicking on the circles corresponding to the modules in the plot automatically updates the ‘Selected Module’ text box below the plot. The user can then locate the module in the map or plot the expected versus actual power output by the module by clicking on the ‘Locate in Map’ and ‘Plot Module Data’ buttons respectively.

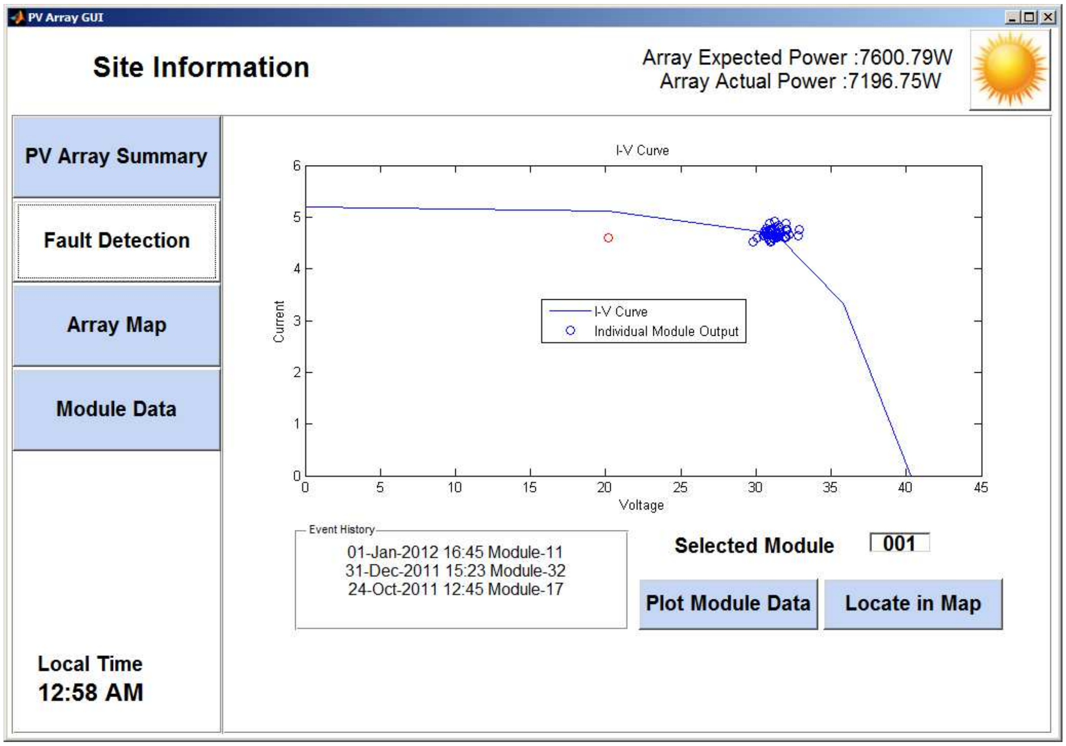

Array Expected Power :7600.79W
Array Actual Power :7196.75W

Event History

01-Jan-2012 16:45 Module-11
31-Dec-2011 15:23 Module-32
24-Oct-2011 12:45 Module-17

Selected Module 001

Local Time
12:58 AM

Figure 4.9: PV GUI: fault detection using MCD algorithm.

4.4 Summary

This chapter discussed the features and visualizations that a module level PV monitoring system can have. This was done by using a demonstration GUI built in MATLAB. Several visualizations which were found to be useful for the array operator to understand the working of array and identify faults were presented. Hourly averages of expected and actual power help the user to identify shading losses in the array. Visualizations were presented for fault detection algorithms that operate on module level data and identify the faulty module and array maps which identify the physical location of the module within the array. Thus the GUI will help monitor the PV array, make sense of the data generated from the monitoring system and find faults. It can be used to improve the performance of the array.

Chapter 5

CONCLUSIONS AND FUTURE WORK

This chapter presents the conclusions reached and potential future work from the sensor configuration simulations and the demonstration GUI.

5.1 Conclusions

The sensor configuration simulations presented in this research are used to quantify the ability of array, string and module level monitoring systems in detecting faults within the array. The effect of monitoring at these locations on detecting ground faults and shading is analyzed. The simulations were performed for the cases where only one module is affected or several modules are affected. Module level sensing performed the best achieving 100 percent fault detection with almost zero false alarms even when only one module is affected by a fault. String level monitoring system performed well only when three or more modules in a string are affected by the fault. For instance, the string level monitoring system cannot detect a ground fault that affects only two modules in the string which corresponds to a 8.4 percent loss in array output power. Array level monitoring system is the worst in detecting faults. Shading and ground faults that affect four or more modules causing well over 20 percent loss of power are not detected. The analysis of the different simulations revealed that current methods of sensing only at the array level results in several potential faults being impossible to detect and most systems require at-least string level monitoring. Module level sensing outperforms string level for every fault case and can detect faults that affect only individual modules. However, since it involves significant number of additional sensors, further study is essential to identify if the better performance justifies the extra sensor overhead.

A demonstration GUI built in MATLAB for visualization of PV array monitoring system with module level sensing data is presented in this work. The GUI accepts input from inverter, individual modules and weather station and provides visualizations to help the user understand the health of the array. Automated fault detection algorithms that run statistics based clustering to identify faults in the array are integrated in to the GUI. Displays are provided to locate the faulty module using a map of the array and plot individual module outputs. These displays can help the user track the health of the PV array and detect faults automatically. Thus they improve the performance of PV.

5.2 Future Work

The sensor configuration simulations were performed with simulated data for ground faults and shading. Other faults can be considered. Faults can be simulated in an actual PV array with module level monitoring system and the performance can be studied. The simulations can be performed for arrays with different number of modules in a series string and the trade-off between module level and string level measurement can be categorised for different string lengths. The cost involved in each type of sensing can be compared with the gains in array performance and sensor locations can be optimized based on cost benefit analysis. The GUI developed can be integrated with algorithms and databases that predict the solar day. This can be used to forecast the output power for each day.

REFERENCES

[1] M. Begovic, S. Ghosh, and A. Rohatgi, “Decade performance of a roof-mounted photovoltaic array,” in *Photovoltaic Energy Conversion, Conference Record of the 2006 IEEE 4th World Conference on*, vol. 2, may 2006, pp. 2383 –2386.

[2] *Solaron 500E HE PV Inverter datasheet*, Advanced Energy Industries, 2011.

[3] M. A. Green, “Short communication: Price/efficiency correlations for 2004 photovoltaic modules,” *Progress in Photovoltaics: Research and Applications*, vol. 13, no. 1, pp. 85–87, 2005.

[4] ——, “Silicon photovoltaic modules: a brief history of the first 50 years,” *Progress in Photovoltaics: Research and Applications*, vol. 13, no. 5, pp. 447–455, 2005.

[5] “Area 1 program summary,” in *Photovoltaic Specialists Conference (PVSC), 2010 35th IEEE*, june 2010, pp. 57 –204.

[6] D. King, W. Boyson, and J. Kratochvil, “Analysis of factors influencing the annual energy production of photovoltaic systems,” *In Proc. Conference Record of the Twenty-Ninth IEEE Photovoltaic Specialists Conference, 2002.*, pp. 1356 – 1361, 2002.

[7] T. Nordmann and L. Clavadetscher, “Understanding temperature effects on PV system performance,” *Proceedings of 3rd World Conference on Photovoltaic Energy Conversion, 2003.*, vol. 3, pp. 2243 –2246, 2003.

[8] D. L. King, J. Kratochvil, and W. Boyson, “Measuring solar spectral and angle-of-incidence effects on photovoltaic modules and solar irradiance sensors,” *Conference Record of the Twenty-Sixth IEEE Photovoltaic Specialists Conference, 1997.*, pp. 1113–1116, 1997.

[9] J. Nelson, *The Physics of Solar Cells*. Imperial College Press, 2003.

[10] C. Honsberg and S. Bowden, *PV CDROM*. [Online]. Available: http://www.pveducation.org/pvcdrom.

[11] W. De Soto, S. Klein, and W. Beckman, “Improvement and validation of a model for photovoltaic array performance,” *Solar Energy*, vol. 80, no. 1, pp. 78 – 88, Aug. 2006.

[12] M. El-Shibini and H. Rakha, “Maximum power point tracking technique,” in *Electrotechnical Conference, 1989. Proceedings. ‘Integrating Research, Indus-*

try and Education in Energy and Communication Engineering', MELECON '89., Mediterranean, 1989, pp. 21 –24.

[13] F. Baumgartner, H. Scholz, A. Breu, and S. Roth, "MPP voltage monitoring to optimise grid connected system design rules," in *Proceedings 19th European Photovoltaic Solar Energy Conference, June*, 2004, pp. 7–11.

[14] I. Altas and A. Sharaf, "A novel on-line MPP search algorithm for PV arrays," *Energy Conversion, IEEE Transactions on*, vol. 11, no. 4, pp. 748 –754, Dec. 1996.

[15] A. Al-Amoudi and L. Zhang, "Application of radial basis function networks for solar-array modelling and maximum power-point prediction," *Generation, Transmission and Distribution, IEEE Proceedings*, vol. 147, no. 5, pp. 310 –316, Sep. 2000.

[16] F. Spertino and J. Akilimali, "Are manufacturing I-V mismatch and reverse currents key factors in large photovoltaic arrays," *IEEE Transactions on Industrial Electronics,*, vol. 56, no. 11, pp. 4520 –4531, Nov. 2009.

[17] R. Hammond, D. Srinivasan, A. Harris, K. Whitfield, and J. Wohlgemuth, "Effects of soiling on PV module and radiometer performance," *Conference Record of the Twenty-Sixth IEEE Photovoltaic Specialists Conference, 1997.*, pp. 1121 –1124, 1997.

[18] H. Patel and V. Agarwal, "MATLAB-Based modeling to study the effects of partial shading on PV array characteristics," *IEEE Transactions on Energy Conversion,*, vol. 23, no. 1, pp. 302 –310, Mar. 2008.

[19] D. Nguyen and B. Lehman, "Modeling and simulation of solar PV arrays under changing illumination conditions," *In Proc. IEEE Workshops on Computers in Power Electronics, 2006. COMPEL '06.*, pp. 295 –299, July 2006.

[20] V. Quaschning and R. Hanitsch, "Numerical simulation of current-voltage characteristics of photovoltaic systems with shaded solar cells," *Solar Energy*, vol. 56, no. 6, 1996.

[21] *NFPA 70: National Electrical Code*, NFPA Std., 2008.

[22] G. Gregory and G. Scott, "The arc-fault circuit interrupter: an emerging product," *IEEE Transactions on Industry Applications*, vol. 34, no. 5, pp. 928 –933, 1998.

[23] H. Haeberlin and M. Kaempfer, "Measurement of damages at bypass diodes by induced voltages and currents in PV modules caused by nearby lightning currents with standard waveform," in *23rd European Photovoltaic Solar Energy Conference*, 2008.

[24] C. Deline, "Partially shaded operation of a grid-tied PV system," in *Photovoltaic Specialists Conference (PVSC), 2009 34th IEEE*, june 2009, pp. 001 268 –001 273.

[25] D. King, J. Kratochvil, and W. Boyson, "Photovoltaic array performance model," Sandia National Laboratory, Tech. Rep., 2004.

[26] *IEEE Std 1547: IEEE Standard for Interconnecting Distributed Resources with Electric Power Systems*, IEEE Std., 2003.

[27] H. Zhiqiang and G. Li, "Research and implementation of microcomputer online fault detection of solar array," in *Computer Science Education, 2009. ICCSE '09. 4th International Conference on*, 25-28 2009, pp. 1052 –1055.

[28] H. Braun, S. T. Buddha, V. Krishnan, C. Tepedelenlioglu, A. Spanias, T. Yeider, and T. Takehara, "Signal processing for fault detection in photovoltaic arrays," in *IEEE Int. Conf. on Acoustics, Speech, and Signal Processing*, 2012, accepted.

[29] E. Dirks, A. Gole, and T. Molinski, "Performance evaluation of a building integrated photovoltaic array using an internet based monitoring system," in *Power Engineering Society General Meeting, 2006. IEEE*, 2006, p. 5 pp.

[30] W. Kolodenny, M. Prorok, T. Zdanowicz, N. Pearsall, and R. Gottschalg, "Applying modern informatics technologies to monitoring photovoltaic (PV) modules and systems," in *Photovoltaic Specialists Conference, 2008. PVSC '08. 33rd IEEE*, May 2008, pp. 1 –5.

[31] M. Zahran, Y. Atia, A. Al-Hussain, and I. El-Sayed, "Labview based monitoring system applied for PV power station," in *Proceedings of the 12th WSEAS international conference on Automatic control, modelling & simulation*, ser. ACMOS'10. Stevens Point, Wisconsin, USA: World Scientific and Engineering Academy and Society (WSEAS), 2010, pp. 65–70.

[32] X. Carcelle, *Power Line Communications in Practice*, 1st ed. Artech House Publishers, 2009.

[33] H. Ferreira, H. Grove, O. Hooijen, and A. Han Vinck, “Power line communications: an overview,” in *AFRICON, 1996., IEEE AFRICON 4th*, vol. 2, 24-27 1996, pp. 558 –563 vol.2.

[34] L. Surhone, M. Timpledon, and S. Marseken, *RS-232: Telecommunication, Data Terminal Equipment, Data Circuit-Terminating Equipment, Serial Port, ITU-T, Electronic Industries Alliance, Asynchronous Serial Communication*. Betascript Publishers, 2010.

[35] D. Gislason, *Zigbee wireless networking*, ser. Safari Books Online. Elsevier, 2008. [Online]. Available: http://books.google.com/books?id=up8Oa7456I8C

[36] F. Chan and H. Calleja, “Reliability: A new approach in design of inverters for pv systems,” in *International Power Electronics Congress, 10th IEEE*, oct. 2006, pp. 1 –6.

[37] D. Ton and W. Bower, “Summary report on the doe high-tech inverter workshop,” US Dept. of Energy, Tech. Rep., 2005.

[38] G. Gregory, K. Wong, and R. Dvorak, “More about arc-fault circuit interrupters,” *IEEE Transactions on Industry Applications,*, vol. 40, no. 4, pp. 1006 – 1011, 2004.

[39] M. Naidu, T. Schoepf, and S. Gopalakrishnan, “Arc fault detection scheme for 42-V automotive dc networks using current shunt,” *IEEE Transactions on Power Electronics,*, vol. 21, no. 3, pp. 633 –639, May 2006.

[40] “EES solver to find the reference parameters of five parameter model.” [Online]. Available: http://sel.me.wisc.edu/software.shtml.

[41] D. King, W. Boyson, B. Hansen, and W. Bower, “Improved accuracy for low-cost solar irradiance sensors,” Sandia National Laboratory, Tech. Rep., 2011.

[42] W. D. De Soto, “Improvement and validation of a model for photovoltaic array performance,” Master’s thesis, University of Wisconsin-Madison, 2004.

[43] P. Cameron, W. Boyson, and M. Daniel, “Comparison of PV system performance-model predictions with measured PV system performance,” Sandia National Laboratory, Tech. Rep., 2008.

APPENDIX A

SANDIA PERFORMANCE MODEL

```
%set module parameters for Sharp NT-175U panel, Sandia model
function [modelParams arrayParams envParams] = get_params()
clear modelParams

modelParams.name = 'Sharp NT-175U1';
modelParams.vintage = 2007;
modelParams.area = 1.3;
modelParams.material = 'c-Si';
modelParams.series_cells = 72;
modelParams.parallel_strings = 1;
modelParams.Isco = 5.40;
modelParams.Voco = 44.4;
modelParams.Impo = 4.95;
modelParams.Vmpo = 35.4;
modelParams.aIsc = .000351;
modelParams.aImp = -.000336;
modelParams.C0 = 1.003;
modelParams.C1 = -.003;
modelParams.BVoco = -.151;
modelParams.mBVoc = 0;
modelParams.BVmpo = -.158;
modelParams.mBVmp = 0;
modelParams.n = 1.323;
modelParams.C2 = .001;
modelParams.C3 = -8.711;
modelParams.A = [.931498305 .059748475 -.010672586 ...
 .000798468 -2.23567E-5];% actual NT-175u parameters
```

```
modelParams.B = [1 -.002438 .0003103 -1.246E-5 2.112E-7 -1.359E-9];
modelParams.dTc = 3;
modelParams.fd = 1;
modelParams.a = -3.56;
modelParams.b = -.075;
modelParams.C4 = .992;
modelParams.C5 = .008;
modelParams.Ixo = 5.32;
modelParams.Ixxo = 3.51;
modelParams.C6 = 1.128;
modelParams.C7 = -.128;
modelParams.e0 = 1000;
modelParams.To = 25;

%%set environmental conditions:
envParams.airmass = 1;
%angle of incidence
envParams.aoi = 0;
envParams.T_ambient = 25;
envParams.T_cell = 30;
envParams.irradiance = 1000;
envParams.P_diffuse = 0;

%%calculates a solar panel IV curve based on the Sandia solar module
%performance model.

function [V I] = get_IV_curve(env, model)
```

```
k = 1.38066E-23; %Boltzmann’s constant, J/K
q = 1.602E-19; % charge of electron, coulombs

%calculate airmass dependence of model:
f_airmass = max(0,polyval(fliplr(model.A),env.airmass));

%calculate angle of incidence dependence:
f_aoi = polyval(fliplr(model.B),env.aoi);

%calculate temperature difference from SRC:
delta_T = env.T_cell - model.To;
%calculate short-circuit current Isc
Isc = model.Isco * f_airmass * (f_aoi * env.irradiance + model.fd ...
* env.P_diffuse)/model.e0 * (1 + model.aIsc*delta_T);

%calculate effective irradiance Ee
Ee = Isc / (model.Isco * (1 + model.aIsc*delta_T));

%calculate maximum-power current Imp
Imp = model.Impo * (model.C0*Ee + model.C1 * Ee^2)*...
(1 + model.aImp*delta_T);

%calculate "thermal voltage" Vt. T_cell converted from C to K
Vt = model.n * k * (env.T_cell + 273.15)/q;

%temperature coefficient as function of effective irradiance
BVoc = model.BVoco + model.mBVoc*(1- Ee);
```

```
%calculate open-circuit voltage Voc
Voc = max(0,model.Voco + model.series_cells*Vt*log(Ee) ...
+ BVoc * delta_T);

%calculate maximum power voltage Vmp
%temperature coefficient as function of effective irradiance
BVmp = model.BVmpo + model.mBVmp*(1- Ee);
Vmp = max(0,model.Vmpo + model.C2*model.series_cells*Vt*log(Ee) ...
+ model.C3*model.series_cells*(Vt * log(Ee))^2 + BVmp * delta_T);

%calculate additional currents Ix and Ixx
Ix = model.Ixo * (model.C4 * Ee + model.C5 * Ee^2)*...
(1 + model.aIsc*delta_T);
Ixx = model.Ixxo * (model.C6 * Ee + model.C7*Ee^2)*...
(1+ model.aImp*delta_T);

%combine points into vectors
V = [0 Voc/2 Vmp (Voc + Vmp)/2 Voc];
I = [Isc Ix Imp Ixx 0];
if V(2) > V(3)
    V = [0 Vmp (Voc + Vmp)/2 Voc];
    I = [Isc Imp Ixx 0];
end
if Voc == 0
    V = 0;
    I = 0;
end
```